doi: 10.1111/sed.13059

Sedimentology (2023) 70, 927-969

# **Keratose sponges in ancient carbonates – A problem of interpretation**

FRITZ NEUWEILER\*, STEPHEN KERSHAW†'‡ (D), FRÉDÉRIC BOULVAIN§, MICHAŁ MATYSIK¶, CONSUELO SENDINO‡, MARK MCMENAMIN\*\* (D) and AXEL MUNNECKE††

\*Département de géologie et de génie géologique, Université Laval, 1065, av. de la Médecine, Québec, OC. G1V 0A6. Canada

†Department of Life Sciences, Brunel University, Uxbridge, UB8 3PH, UK (E-mail: stephen.kershaw@brunel.ac.uk)

‡Earth Sciences Department, The Natural History Museum, Cromwell Road, London, SW7 5BD, UK §Pétrologie Sédimentaire, Université de Liège, Quartier Agora, B20, Allée du six Août, 12, Sart Tilman, B-4000, Liège, Belgium

¶Institute of Geological Sciences, Jagiellonian University, Gronostajowa 3a, 30-387, Kraków, Poland \*\*Department of Geology and Geography, Mount Holyoke College, 50 College Street, South Hadley, MA, 01075, USA

††GeoZentrum Nordbayern, Fachgruppe Paläoumwelt, Friedrich-Alexander-Universität Erlangen-Nürnberg (FAU), Loewenichstraße 28, D-91054, Erlangen, Germany

Associate Editor - Giovanna Della Porta

#### ABSTRACT

Reports of diverse vermiform and peloidal structures in Neoproterozoic to Mesozoic open marine to peritidal carbonates include cases interpreted to be keratose sponges. However, living keratose sponges have elaborate, highly elastic skeletons of spongin (a mesoscopic end-member of a hierarchical assemblage of collagenous structures) lacking spicules, thus have poor preservation potential in contrast to the more easily fossilized spiculebearing sponges. Such interpreted fossil keratose sponges comprise diverse layered, network, amalgamated, granular and variegated microfabrics of narrow curved, branching, vesicular-cellular to irregular areas of calcite cement, thought to represent former spongin, embedded in microcrystalline to peloidal carbonate. Interpreted keratose sponges are presented in publications almost entirely in two-dimensional (thin section) studies, usually displayed normal to bedding, lacking mesoscopic three-dimensional views in support of a sponge body fossil. For these structures to be keratose sponges critically requires conversion of the spongin skeleton into the calcite cement component, under shallow-burial conditions and this must have occurred prior to compaction. However, there is no robust petrographic-geochemical evidence that the fine-grained carbonate component originated from sponge mummification (automicritic body fossils via calcification of structural tissue components) because in the majority of cases the fine-grained component is homogenous and thus likely to be deposited sediment. Thus, despite numerous studies, verification of fossil keratose sponges is lacking. Although some may be sponges, all can be otherwise explained. Alternatives include: (i) meiofaunal activity; (ii) layered microbial (spongiostromate) accretion; (iii) sedimentary peloidal to clotted micrites; (iv) fluid escape and capture resulting in bird's eye to vuggy porosities; and (v) moulds of siliceous sponge spicules. Uncertainty of keratose sponge identification is fundamental and far-reaching for understanding: (i) microfacies and diagenesis where

#### 928 F. Neuweiler et al.

they occur; (ii) fossil assemblages; and (iii) wider aspects of origins of animal clades, sponge ecology, evolution and the systemic recovery from mass extinctions. Thus, alternative explanations must be considered.

**Keywords** Automicrite, metazoan evolution, microfacies analysis, mummification, sponge taphonomy.

#### INTRODUCTION

This study addresses problems of reliable recognition of fossil keratose sponges in shallowmarine limestones and dolostones, an issue based on a variety of microfabrics, advocated as sponges at the scale of microfacies (thin sections). For this investigation, sponges present two fundamental forms requiring understanding in relation to preservation as fossils: (i) those lacking mineral parts constituting (among others) the Keratosa group of demosponges (Fig. 1A to D); and (ii) those with opaline mineral spiculate skeletons (Figs 1E, 1F, 2A, 2B, 3, 4 and 5A to D). This topic is important because claims of keratose sponges relate to accuracy of microfacies analysis and might extend the fossil record of aspiculate demosponges deep into the Neoproterozoic (Turner, 2021). Analysis of these structures therefore affects fundamental understanding of sedimentary facies containing such microfabrics across a long-time range and, at its extreme (Turner, 2021), presents a profound contradiction with modelled molecular divergence time estimates of respective clades (Fig. 2; Schuster et al., 2018; Kenny et al., 2020). The best-known fossil aspiculate(?) sponge, the ?verongid Vauxia (Fig. 5E and F) contains chitin, not spongin (Ehrlich et al., 2013); and the former presence of opaline spicules is a matter of debate (Yang et al., 2017; Fan et al., 2021). Vauxiids might relate to latest stem-group demosponges, some of the earliest heteroscleromorphs (with spicules), and early verongids (without spicules), outlined by Botting et al. (2013). Indeed, lack of spicules creates uncertainty in the phylogenetic position of sponges, discussed by Maldonado (2009). Study of mineral spiculate sponge skeletons commonly begins with hand specimens (e.g. De Freitas, 1991; Pisera, 1997; Rigby et al., 2008; Botting et al., 2017) either as body fossils or disaggregated spicules, noting that on death modern sponges generally decay very quickly, opaline spicules readily dissolve, and in many instances leave no record (Debrenne, 1999; Wulff, 2016).

The fossil record shows evidence of early evolution and diversification of spiculate sponges from exceptional preservation of Cambrian and Ordovician sponges (Carrera & Botting, 2008; Botting & Muir, 2018), and the estimated origin of sponges is supplemented by molecular clock phylogeny considering multiple calibration sets (Dohrmann & Wörheide, 2017; Schuster et al., 2018; Kenny et al., 2020). Problematically, fossil sponges with mineral skeletons assessed solely from thin sections are impossible to identify with sufficient taxonomic detail, particularly if disaggregated (see Flügel, 2004, p. 495, 799) because spicule shape and size can be difficult to determine, or are obscured by pervasive recrystallization (that may or may not be cathodoluminescence microresolved with scopy). Some secondary abiogenic mineral precipitates have been mistaken for sponge spicules in thin section (Antcliffe et al., 2014).

Fossilization of keratose (aspiculate) sponges is significantly more problematic than for biomineralic sponges because of the issue of preserving the spongin organic skeleton in marine carbonates. Nevertheless, keratose sponges have been inferred in a range of facies from restricted lagoons to open shelf, thus relatively shallow facies. Interpretations of fossil keratose sponges in carbonates began with Szulc (1997) in stromatolites from restricted lagoonal facies (Matysik, 2016) in Middle Triassic Muschelkalk carbonates from Upper Silesia (Poland) (Figs 6 and 7). Szulc (1997) inferred that pockets and layers of porous micrite within the stromatolites are sponges, but did not give criteria for recognition of sponges, noting that the porous structures described do not represent spicules (Figs 6 and 7). Szulc (1997) noted similar deposits from Thuringia (central Germany) that are silicified, from which Szulc inferred that the proposed sponges were siliceous. Non-spiculate sponges were inferred by Reitner et al. (2001) and Reitner & Wörheide (2002, fig. 10) for Devonian mud-mounds (Boulonnais, France). Then, in a landmark study, Luo & Reitner (2014) re-used Triassic and Devonian material in serial grinding and imaging

methods to construct microscopic 3D views, proposing presence of fossil keratose (aspiculate) sponges. However, Luo & Reitner (2014) themselves realized the uncertainty of sponge interpretation, with terms such as 'most likely' and 'putative'. Luo & Reitner's (2014) work was developed by Luo & Reitner (2016), and these studies were subsequently used to support numerous proposals of keratose sponges in thin sections of other carbonates from Neoproterozoic to at least Triassic time (see compilation of publications in Table S1). Key examples are by Reitner et al. (2001), Luo & Reitner (2014, 2016), Lee & Hong (2019), Lee & Riding (2021a,b, 2022, 2023), Baud et al. (2021), Pei et al. (2021a,b), Pham et al. (2021), Gischler et al. (2021), Turner (2021) and Reitner et al. (2021). Luo et al. (2022) presented criteria for recognition of fossil keratose sponges, which are discussed later. No published cases of vermiform structure interpreted as sponges in rocks younger than Jurassic were found during this study, although Luo (2015, p. 100-103) argued that possible keratosan sponges occur in Cretaceous and Eocene strata.

The problem of interpretation of keratose sponges is lack of reliable criteria for identification of their fossilized remains in any part of the rock record; and there is no known diagenetic process that could transform: (i) the spongin skeleton into sparitic calcite commonly described as keratose sponge structure; and (ii) the canalbearing soft tissue between the spongin skeleton (Fig. 2C and D) into largely homogenous microcrystalline carbonate that dominates space between sparite networks of interpreted keratosans. In contrast, for biomineralic (siliceous) sponges, Figs 3, 4 and 5A to D show the types of preservation commonly encountered in thin section. They largely comprise a distinct network of spar-cemented spicule moulds that subsequently might recrystallize, but in some cases also display a former sponge canal system due to automicrite production (= mummification; Fig. 3; Neuweiler et al., 2007, for short review).

Interpreted keratose sponges in carbonate rocks may instead be viewed diversely as problematica (definite fossils, with unknown affinities), fragments of altered siliceous sponges, graphoglyptid trace fossils or even dubiofossils to pseudofossils. Two main issues need resolving: (i) assessment of arrangement of components of interpreted keratose sponges; and (ii) consideration of alternatives for future research. First, a background review is presented, addressing issues of fossil sponges that necessarily involves description of

relevant features of modern sponges. Then classification, description and discussion of the range of microfabrics of interpreted keratose sponges in carbonate rocks is explored. The focus is on four key settings containing possible keratose sponges: Neoproterozoic carbonates; close associations of stromatolites and sponges (Cambrian, Triassic); Cambro-Ordovician carbonates; and carbonate facies in the aftermath of the end-Permian mass extinction.

#### **BACKGROUND REVIEW**

Ambiguities in interpretation and classification of sedimentary carbonate materials are widespread, mostly related to the structure and voluimportance of relatively microcrystalline grains (Lokier & Al Junaibi, 2016). Sources of error include problems of identification in thin-section of structures that may be fossils, in terms of form, functional design and skeletal microstructure (Knoll, 2003; Flügel, 2004), constituting a grey zone between clearly identifiable and suspect structures. This grey zone comprises three types of objects: (i) biogenic but requiring interpretation of basic taxonomic placement (Problematica sensu lato; Jenner & Littlewood, 2008; for example, Palaeozoic Halysis as red alga, cyanobacteria, green alga or tabulate coral; Zheng et al., 2020); (ii) distinct structures that are inconclusive in terms of biogenicity (dubiofossils of Hofmann, 1972); and (iii) distinct structures that are certainly abiotic in nature (pseudofossils, discussion in McMahon et al., 2021). Another aspect is that the granularity of carbonate deposits may be post-depositional in nature due to meiofaunal to endofaunal activity, localized microburrow nests or even diagenesis (Debrenne et al., 1989; Wood et al., 1993; Pemberton & Gingras, 2005; Löhr & Kennedy, 2015; McMenamin, 2016; Wright & Barnett, 2020). Furthermore, this grey zone applies to cases extending into deep time and even touches exobiology (Cloud, 1973; for example, biogenicity criteria for tubular filaments and lamination; chemical gardens comprising inorganic processes resulting in structures resembling organisms; molar-tooth structures; see Grotzinger & Rothman, 1996; Awramik & Grey, 2005; McMahon et al., 2017, 2021; McMahon & Cosmidis, 2021). This range of fabrics persists throughout the Phanerozoic in various ways. Examples are: biogenicity of stromatactis (shown partially in Fig. 4B) and lamination (Bathurst,

## 930 F. Neuweiler et al.

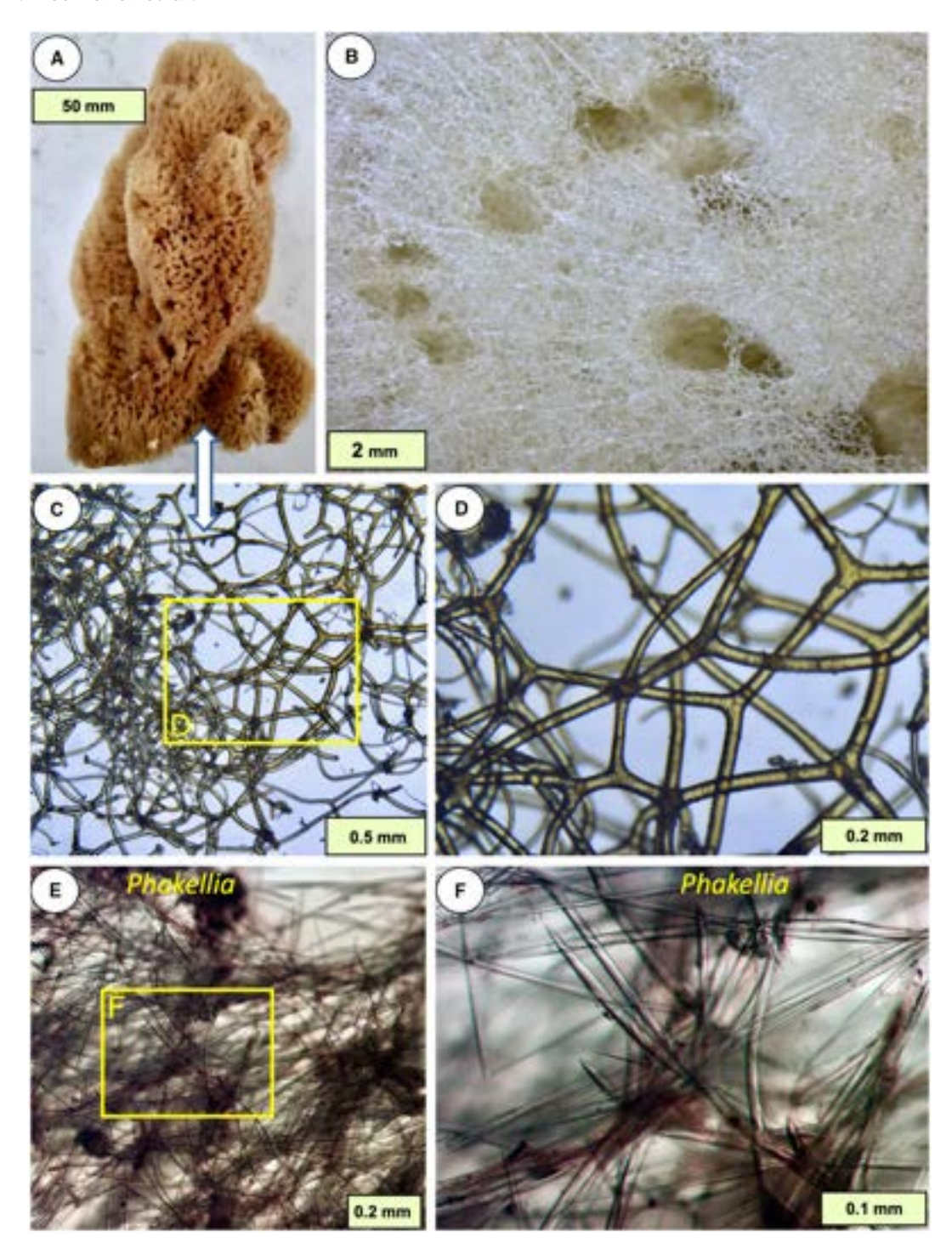


Fig. 1. Examples of modern spongin-bearing sponges. (A) Side view of a modern commercial keratose sponge (Spongiidae Gray, 1867 cf. Spongia) consisting of only spongin (all soft tissue removed) showing that its form is maintained by an elastic spongin network. (B) Detail of Spongia sp. (vertical cut) showing hierarchical set of spongin network fibres and a mesoscopic sponge canal system. (C) and (D) Detail of (A) showing spongin network architecture, with branches and curved form. (E) and (F) Skeletal structure of heteroscleromorph demosponge Phakellia robusta Bowerbank displaying opaline spicules encased by small amounts of spongin (brownish); Shetland, Scotland. Bowerbank collection, Natural History Museum, London, sample, NHMUK 1877.5.21.420.

1982; Bourque & Gignac, 1983; Bourque & Boulvain, 1993; Awramik & Grey, 2005; McMahon et al., 2021); formation of peloids and pelletoids (Fig. 3E; Bourque & Gignac, 1983; Macintyre, 1985); significance of the polymud fabric (Lees & Miller, 1995; Neuweiler et al., 2009); or some drag marks, Rutgersella and Frutexites (Cloud, 1973; Retallack, 2015; McMahon et al., 2021).

In the last decade, molecular phylogenetic studies have shed new light on the traditional taxonomic and phylogenetic framework of sponges, revealing or confirming several polyphyletic groups, establishing new clades, and constraining respective divergence-time estimates (Erpenbeck et al., 2012; Gazave et al., 2012; Morrow & Cárdenas, 2015; Schuster et al., 2018; Kenny et al., 2020), see Fig. 2E. A valuable general reference for sponge groups is de Voogd et al. (2022). Spongin is considered to have evolved in close association within the demosponge lineage (Morrow & Cárdenas, 2015). Sponge spicules may not represent an essential character of early sponge evolution (Ax, 1996; Botting & Muir, 2018, for an alternative view), and were secondarily lost in a multiple and convergent manner (Fig. 2E). Keratose sponges are distinguished from other aspiculate demosponges (Verongimorpha, some Heteroscleromorpha according to Erpenbeck et al., 2012) at the cellular level in combination with details or even absence of an elaborate spongin skeleton (Erpenbeck et al., 2012).

Secure identification of fossil sponges essentially relies on spicules, identified according to their specific design and arrangement, comprising: form, orientation, assemblage and mineralogy (examples in Figs 1 to 4). Although sponges may be preserved as silica and pyrite and in concretions (presumably in low oxygen preservational conditions), of great importance in this study is preservation via a process called mummification: early calcification (thus lithification) of structural tissue components with their associated sediment, to preserve the shape and organization sufficient to allow recognition as a sponge (canal system, preservation of non-rigid spicular architecture; Fritz, 1958; Bourque & Gignac, 1983; Reitner & Keupp, 1991; Pisera, 1997; Neuweiler et al., 1999; Reitner & Wörheide, 2002; Neuweiler et al., 2007, for short review), see Fig. 3. In other cases, there are specific secondary calcareous skeletons that leave a good record, for example, stromatoporoids, chaetetids, inozoans and sphinctozoans, at least one of which (Vaceletia) is

coralline keratose considered а sponge (Wörheide, 2008). Some sponges leave distinct ichnofossils (Entobia), that may contain spicule evidence of their formation (Reitner & Keupp, 1991; Bromley & Schönberg, 2008). Biomarkers might be of additional value (e.g. Love et al., 2009), but their study requires detailed understanding of both history of fluid flow and molecanalogues of possible other (Erpenbeck & van Soest, 2007; Antcliffe et al., 2014). More recently, the entire biomarker approach to try to conclude for a sponge-specific origin was called into question (Nettersheim et al., 2019; Bobrovskiy et al., 2020). Confusingly, some foraminifera use sponge spicules to agglutinate their tests (Rützler & Richardson, 1996; Kamenskaya et al., 2015). Furthermore, some trace fossils in siliceous spiculites are surrounded by brighter rings of densely packed spicules (Matysik et al., 2018, 2021) that, although in some cases resemble sponges by having a central canal surrounded by a body-like ring, are interpreted to have been produced due to parapodial sorting of spicules by the trace-making organism (Goldring et al., 1991). Such structures need careful examination to be distinguished from sponges.

Because of the non-mineral composition of modern aspiculate sponges (Keratosa and Verongimorpha) with their complex, hierarchical assemblage of various collagenous structures (Manconi et al., 2013, 2022; Stocchino et al., 2021), potential for their preservation as fossils is highly problematic. Body shape stability of keratose sponges (Fig. 1A and B) primarily relies on fibrillar to amorphous collagen as a key component of their extracellular collagenous matrix (ECM; in support of cellular cohesion; Manconi et al., 2022), that at microscale to mesoscale is combined with a highly elastic and elaborate organic skeleton composed of the non-fibrillar (commonly filamentous) collagen spongin, in support of shape-sustaining growth (Junqua et al., 1974; Garrone, 1978; Exposito et al., 1991; Erpenbeck et al., 2012; Manconi et al., 2013, 2022; Ehrlich et al., 2018; Ehrlich, 2019). Indeed, the fossil record of non-spiculate sponges was described by Reitner & Wörheide (2002) as being poor, noting that vauxiid sponges of the middle Cambrian Burgess Shale are the best examples (Fig. 5E and F), in lowoxygen preservation, contrasting the oxygenated environments of proposed keratose sponges considered in this study. However, Ehrlich et al. (2013) revealed that those vauxiid sponges

some evolve elaborate spongin-spicule skeletons

1365991, 2023, 3. Downloaded from https://onlinelibtrary.wiley.com/doi/10.1111/sed.13095 by Mount Holyoke College Library, Wiley Online Library on [02/01/2024]. See the Terms and Conditions (https://onlinelibtrary.wiley.com/terms-and-conditions) on Wiley Online Library for rules of use; OA articles are governed by the applicable Creative Commons

Fig. 2. Examples of two modern sponges demonstrating more diversity of sponge architecture. (A) and (B) Heteroscleromorph demosponge *Axinella verrucosa* Esper, from the Adriatic Sea, showing similar amounts of spongin (yellow arrow) and opaline spicules (orange arrow). Spicules are embedded within, or echinate off, the spongin. Bowerbank collection, Natural History Museum, London, sample NHMUK 1877.5.21.1239. (C) and (D) Microtome sections of keratose sponge *Ircinia* (Joulters Cay, The Bahamas) showing a specific kind of mesoscopic spongin (with pith and bark; yellow arrow) locally containing agglutinated sedimentary particles (red arrow in D). Soft tissue organization (mesohyl, orange arrow) with canal system (blue arrow). Purple arrow in (D) refers to choanocyte chambers. If the spongin component is to be fossilized, then it may be expected that fossil sponges comprising spongin with skeletal (A and B) or agglutinated particles (C and D) should show both components, but this has not yet been demonstrated. (E) Summary of the evolutionary history of sponges (compiled from Schuster *et al.*, 2018; Kenny *et al.*, 2020), drawing attention to major events of taxa in scope and the multiple (convergent) loss of opaline spicules within demosponges (aspiculate sponges, including Keratosa).

contain chitin (as fungi, other sponges and a number of invertebrates do), but spongin was not detected. Fan *et al.* (2021) classified aspiculate vauxiid sponges in the Chengjiang biota (early Cambrian) as keratose sponges, preserved in partly silicified form. Complexity in phylogeny of early Cambrian sponges was shown by Botting *et al.* (2013), regarding both spiculate and aspiculate taxa.

Apart from vauxiids noted above, literature search revealed no verified cases of potential candidates of fossil keratose sponges in the entire rock record. Important in modern spiculate sponges are variable amounts of nonspicular material in proportion to spicule content. Thus, detailed features of sponges with and without spicules are needed. Figure 2A and B show details of a modern heteroscleromorph spiculate demosponge representing the common occurrence of tightly connected opaline spicules and mesoscopic spongin fibres known for many decades (Axinellidae, Carter, 1875), yet there is no proof of a respective fossil in thin section representing such a distinct composite skeletal architecture, noting that Botting et al. (2013) illustrated orientated spicules in sponge masses presumed to have been embedded in spongin that is not directly observed. Singular claims for fossil Axinellidae are unconfirmed (Reitner & Wörheide, 2002, fig. 9, which may instead be spicule-preserving Entobia). Also, modern keratose sponges may comprise conspicuous primary fibres of spongin up to 250 µm thick and distinctively cored by sand grains (Irciniidae, Gray, 1867; see also Manconi et al., 2013, 2022) (Fig. 2C and D) but, again, there is no respective fossil record. For further comparison, Figs 3F to H and 5A to D demonstrate carbonate fabrics typical of preserved spicule-bearing sponges, but to the best

of the authors' knowledge, there are no examples in carbonate rocks of fossil spiculate demosponges with a proven spongin component (presumed lost in decay and diagenesis). Such details are important for understanding of how sponges might be preserved (Pisera, 2004, for short review), and comparisons between these and fossil cases are made later in this paper. Nevertheless Botting's (2005) description of sponges in volcanogenic sandstones of the Middle Ordovician Llandegley lagerstätte interpreted silicified spongin to maintain the sponge fossil coherence, evidence that spongin preservation is possible, but not yet verified for carbonates. Criteria for distinguishing, example, carbonate microfabrics attributed to sponges from microbial deposits in ancient carbonates (Wallace et al., 2014; Shen & Neuweiler, 2018) are among possible interpretations explored in this study.

## MATERIAL AND METHODS

Samples from several stratigraphic intervals, of authors' own collections and museum material, are used to assess interpretations of keratose sponges. Authors' material comes from: Cambrian and Ordovician of North China; Cambro-Ordovician of Nevada and Utah (USA); Silurian of Canada and south China; Devonian of Belgium; Viséan of Boulonnais region (France); Triassic of the Upper Silesian region (Poland) including some original samples from Triassic localities from Poland and Israel used by Szulc (1997) and Luo & Reitner (2014, 2016); and Cretaceous of Spain. Examination was made of the original spongiostromate material (Visé Group, Namur region) of Gürich (1906) stored at the Royal Belgian Institute of Natural Sciences

#### 934 F. Neuweiler et al.

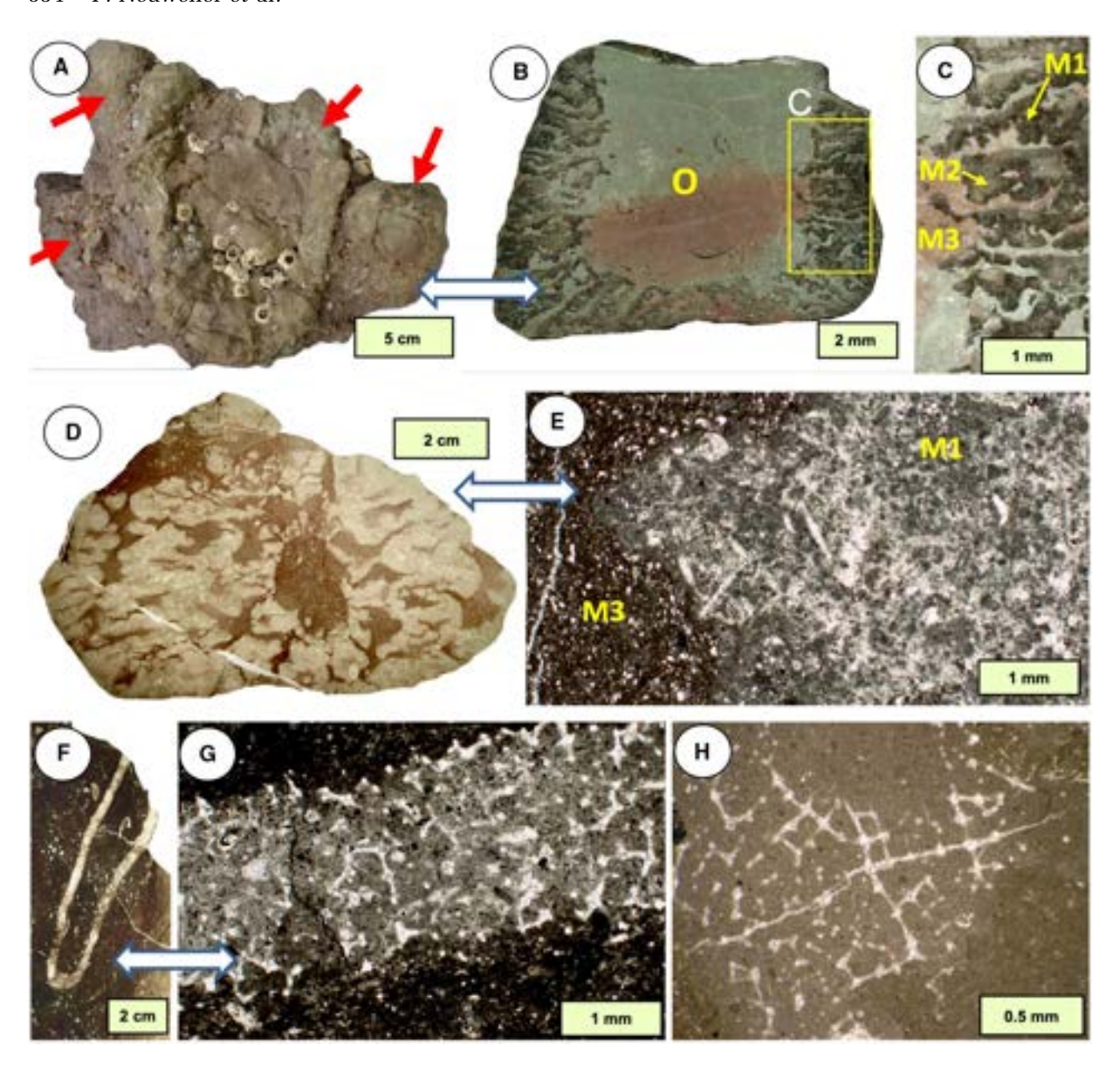


Fig. 3. Examples of fossil sponge mummies. (A) to (E) Malumispongium [hexactinellid, non-rigid (lyssacine) spicule-poor]; Lower Silurian La Vieille Formation, Gaspé Peninsula, Canada (Bourque & Gignac, 1983). (A) Several Malumispongium (red arrows; note modern encrusting barnacles on coastal outcrop). (B) Polished slab of Malumispongium preserving structural tissue components [canal system, osculum (o)]. (C) Detail of (B) displaying dark, gravity-defying automicrite (M1), dark-grey geopetal allomicrite M2 deposited in sponge canals and final matrix of argillaceous silty limestone (M3). (D) Transverse thin section of Malumispongium with canal system and central osculum (o). (E) Enlargement of (D) showing sharp-edged distinction between M1 and M3. M1 (automicrite) displays pelletoidal (authigenic) microfabric locally preserving calcite-cemented moulds of opaline spicules. (F) and (G) Mummified hexactinellid with rigid (lychniscose) skeleton, Cretaceous (Albian), Soba Valley, northern Spain. (F) Thin-section of sponge body. (G) Detail of (F) with local automicrite production confined to sponge, contrasting argillaceous sedimentary host, thus mummified on the ancient sea-floor. (H) For comparison, non-mummified fragment of hexactinellid lacking distinction between sedimentary host and intraskeletal matrix (Dalichai Formation, Bajocian–Callovian (Jurassic), Alborz Mountains, northern Iran); image from Andrej Pisera.

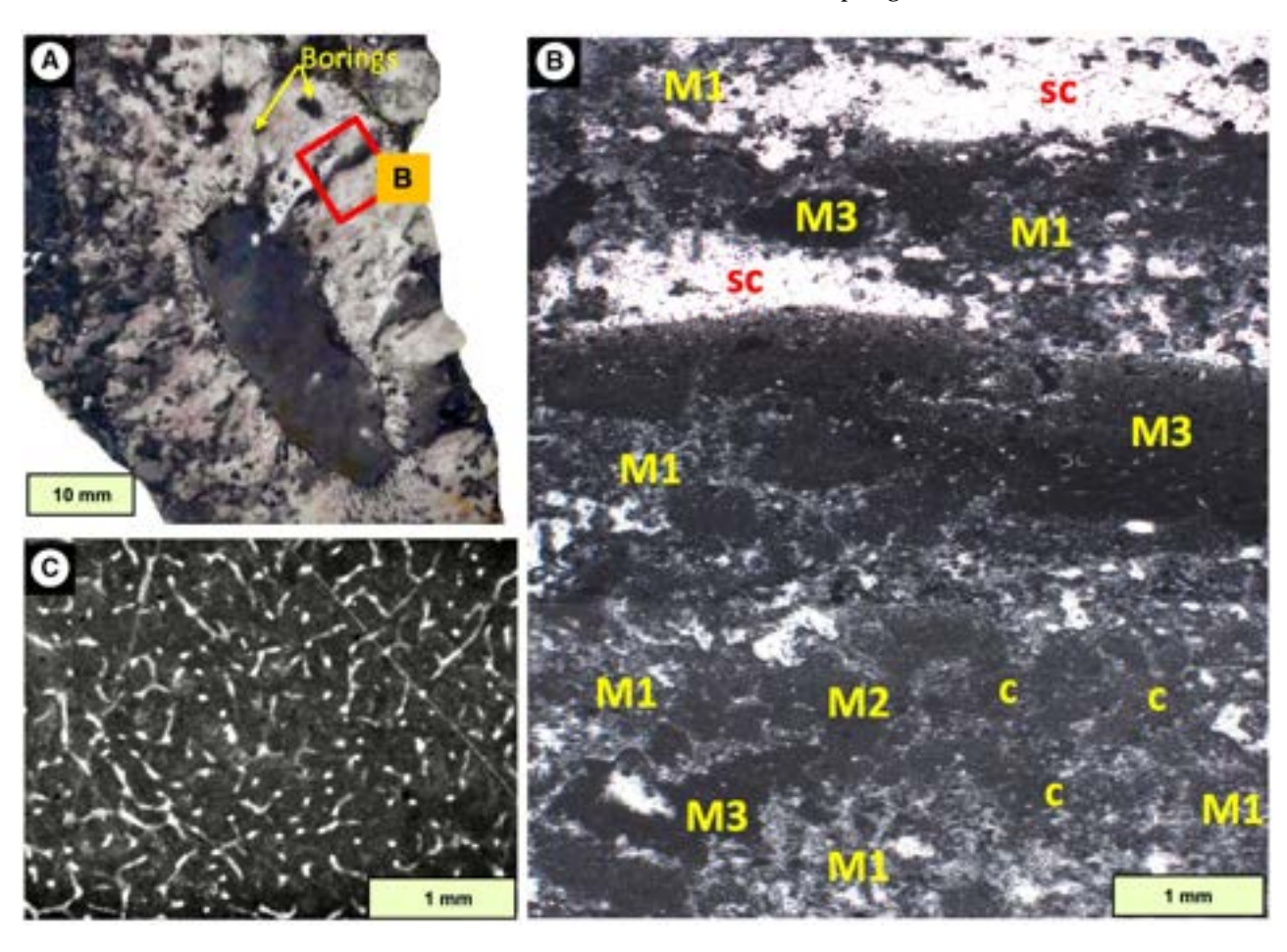


Fig. 4. (A) and (B) Partially mummified lithistid demosponge, Cretaceous (Albian), Soba Valley, northern Spain. (A) Transverse thin-section shows incomplete mummification (= pelletoidal automicrite) enclosing the desmataspicular architecture labelled as M1 in (B), remnants of canal system and centripetally-orientated borings into the sponge, indicating sea-floor exposure of mummy. (B) Enlargement of red box in (A) showing structural-textural complexity of mummification, in contrast to the homogenous micrite observed in interpreted fossil keratose sponges. M1: calcite-cemented moulds of desmata enclosed by pelletoidal automicrite; M2: infiltrated sediment represents the canal system (c). Where neither mummification nor sediment infiltration occurred, dissolution of opaline skeleton produced secondary cavities (sc) subsequently infiltrated by M3 (slightly darker grey than M2, with ostracods and small intraclasts). M3 also occluded borings of irregular outline cross-cutting M1. (C) Duplicated image of interpreted Late Ordovician keratose sponge from Lee & Riding (2021a, fig. 8C), demonstrating homogenous micrite infill between network sparite, contrasting mummified sponge tissue in (B). Reproduced under Creative Commons licence (http://creativecommons.org/licenses/by/4.0/). See text for discussion.

(Brussels) and a selection of modern spiculate and non-spiculate sponges illustrated by Bowerbank (1862) stored at the Natural History Museum London (UK). The New York State Museum (Albany, USA) provided access to original samples (Goldring, 1938) of Cryptozoön stromatolites from its type locality (Hoyt Limestone of the Little Falls Formation, Cambrian) in reference to keratose sponge interpretations presented by Lee & Riding (2021a,b). Polished rock samples and thin sections were studied under plane-polarized (PPL) and cross-

polarized (XPL) light, supplemented with selected cathodoluminescence (CL) and ultraviolet (UV) fluorescence views. For histological microtome sections (*Ircinia*, The Bahamas), the methods and sampling site of Neuweiler *et al.* (2007) apply.

Carbonate terminology is an area of complexity because of the ease with which precipitated and cemented calcium carbonate can be dissolved and recrystallized, so that the sizes of crystals within deposited and recrystallized carbonate overlaps the sizes of precipitated cement

#### 936 F. Neuweiler et al.

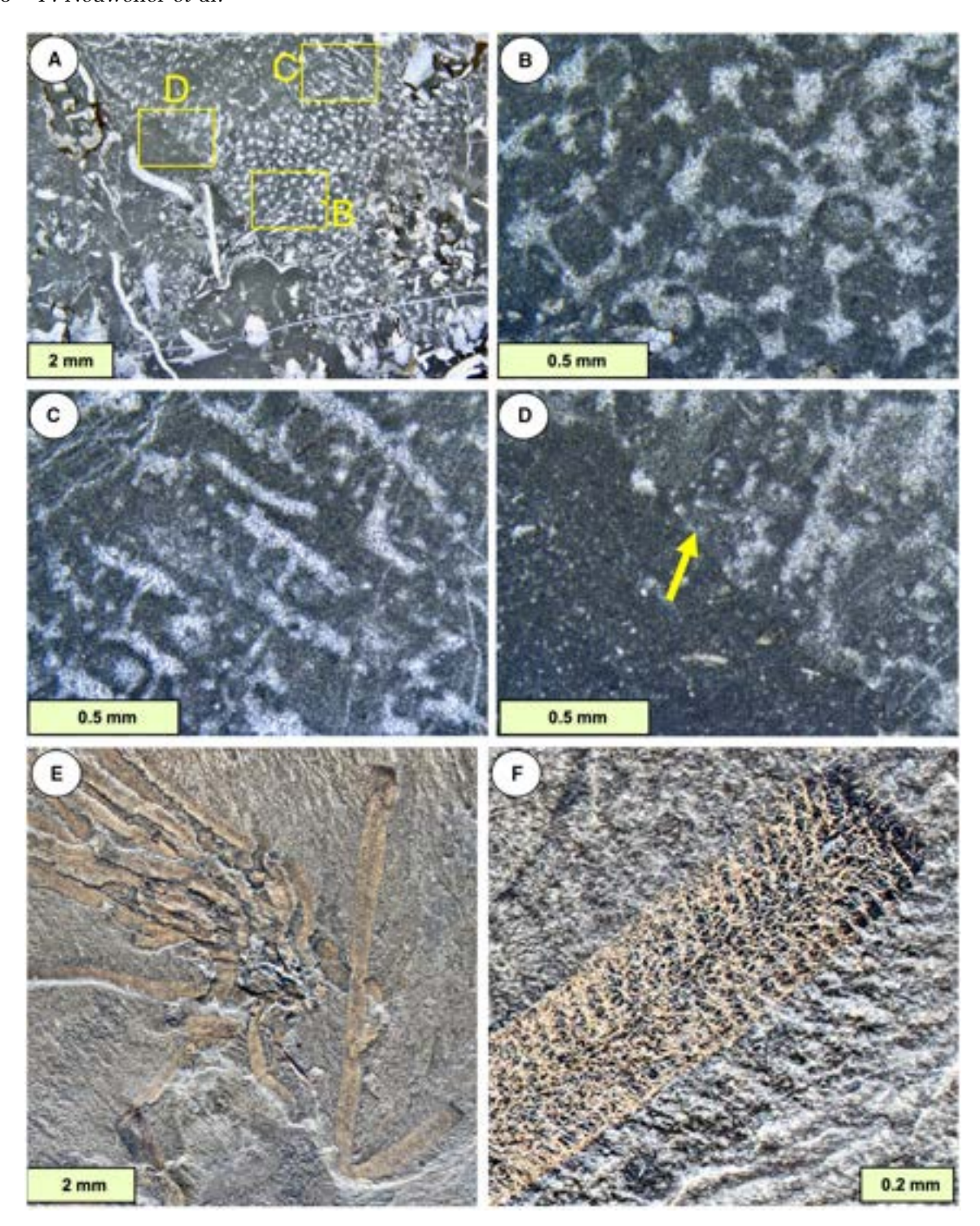


Fig. 5. Palaeozoic sponges as observed in thin section (A) to (D) and as surface relief (E) and (F); Vauxia. (A) to (D) Lithistid calcified spiculate sponges showing rectilinear network structure. (A) The sponge forms a discrete object in the upper right half, locations of (B) to (D) are indicated. (B) and (C) Details of transverse (B) and vertical (C) sections of spiculate structure, noting spicules are preserved as calcite-cemented moulds. (D) Detail of sponge margin showing sharp cortical contact (arrow) with surrounding matrix sediment. Church Reef, Filimore Formation, L. Ordovician, Utah. (E) and (F) Aspiculate fossil sponge Vauxia gracilenta Walcott, 1920 from the Burgess Shale, regarded as one of the best examples of fossil aspiculate, possibly keratose sponges, see Walcott (1917). Specimen NHMUK PI S3071 in the Natural History Museum, London.

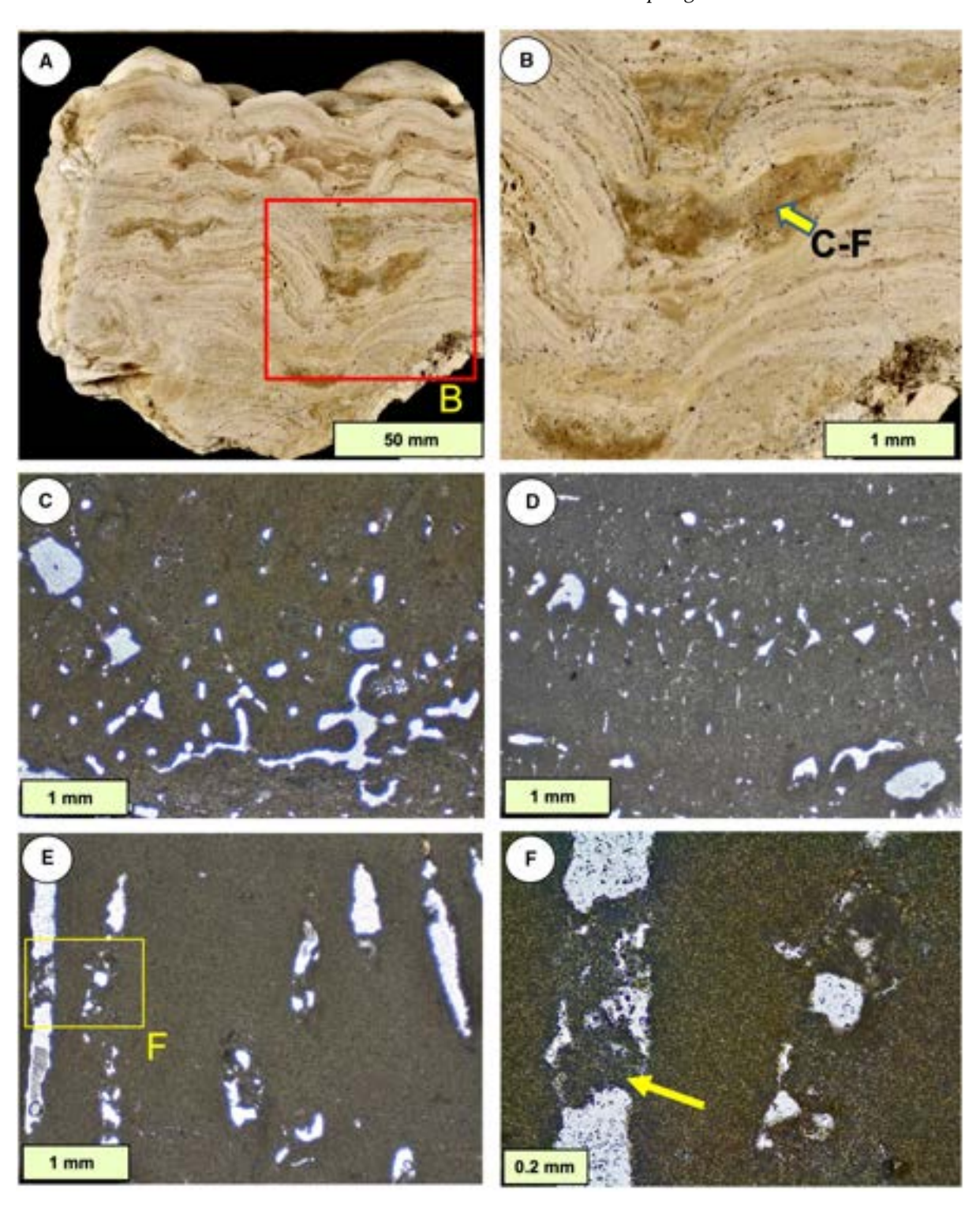
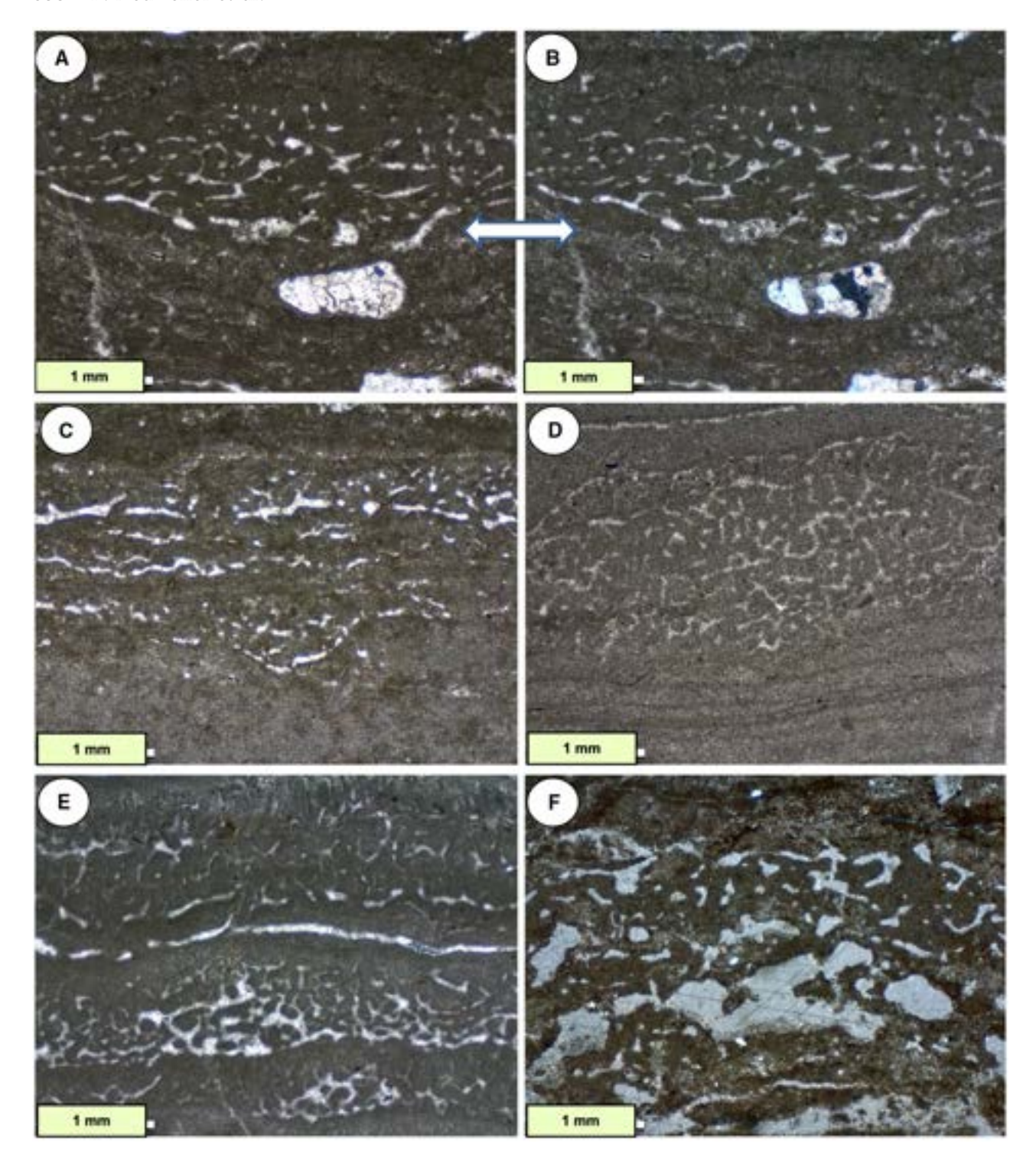


Fig. 6. Stromatolite samples from material proposed by Szulc (1997) to contain sponges; compare with Figs 7 and 8. (A) and (B) Vertical sections showing interlayered sediment in which porous fabrics (yellow arrow) were considered as sponge by Szulc. (C) and (D) Vertical thin section views of interlayered sediment in (A) and (B), showing organized porosity as subvertical voids. (E) and (F) Detail of one of numerous pores showing partial infill with dolomicrite (yellow arrow); the irregular infills are in local continuity with enclosing host rock, implying dissolution-enhanced primary porosity and thus not consistent with interpretation as permineralized sponge. From collections of Joachim Szulc; boundary between *Diplora* Beds and overlying Tarnowice Beds, Muschelkalk, Middle Triassic, Libiaż Quarry, Upper Silesia, Poland. The sample illustrated here is one used by Szulc (1997).



**Fig. 7.** More stromatolite samples from material studied by Szulc (1997) in his proposal that they contain sponges. Compare with Fig. 6 and Luo & Reitner (2014, 2016) to appreciate the range of vermiform fabrics present in these deposits. Such microfabrics conventionally are ascribed to spongiostromata locally containing vugs and fenestrae. (E) Note distinct biolamination defined by subhorizontal to subvertical textures.

crystals (Folk, 1965; Bathurst, 1975; Flügel, 2004). Thus the term 'microcrystalline' is applied to both deposited sediment and cement in appropriate places in this paper. In this study, carbonate materials are considered in two forms:

1 Areas of light-coloured crystalline carbonate clearly visible under light microscopy, comprising both precipitated cement and recrystallized former fabrics in different samples. Some is sparite (>62 microns, Folk, 1965), generally considered to be pore-filling cement, but much of it is smaller, then representing microsparite, applied to both small-scale pore-filling cements and recrystallized micrite (also compare Munnecke *et al.*, 1997, and Flügel, 2004, p. 94–95).

2 Between light-coloured cements is darker-coloured, finer-grained carbonate comprising a mixture (using the size definitions of Folk, 1965) of micrite (<4 microns), microspar (4–30 microns) and pseudospar (>30 microns), the latter two being recrystallized sediment, not pore-filling cement. This material commonly forms a homogenous texture, consistent with sediment fill. In some cases, such material may show clotted to granular–pelletoidal fabrics (i.e. grains are distinguishable in contrast to clotted, where grains merge) consistent with a fine-crystalline component precipitated at or near the sea-floor (automicrite).

## **RESULTS**

From thin sections of primary material and in literature, this study recognizes five broad fabric categories of structures that have been interpreted as fossil keratose sponge, differing in context, architecture and microstructure. These five categories encompass layered, network, amalgamated, granular and variegated fabrics, with some overlap; thus some examples fit into more than one category. In some cases reported in literature, the fabrics occur within shells but not in matrix surrounding shells (Park et al., 2017, fig. 3) or occur in discrete patches in micrite and may have been burrows (Park et al., 2015, fig. 4D); these two cases may reflect re-burrowing of organic-rich sediment encased in pre-existing burrows and shells. Many other examples occur within earlyformed cavities in early-lithified limestone (Lee et al., 2014). In addition to published twodimensional thin section studies is work by Luo & Reitner (2014) and Luo et al. (2022) that

provides preliminary three-dimensional reconstructions at microscopic scale. These limited studies are an important step forward and future work (3D at mesoscopic scale) may help to resolve the nature of the five categories considered here. Thin sections made thicker than normal also give an indication of 3D structure but are limited in value.

In the following sections (see Figs 6 to 20), according to the ideas of keratose sponge interpretation, curved and irregular microsparite to sparite patches represent the position of original spongin structures and the microcrystalline infill represents location of other prior sponge soft tissue. Clearly, of great importance is to explain how: (i) keratosan sponges could be preserved through biostratinomic and diagenetic processes that began with an elaborate organic skeleton made of spongin enveloped by a canal-bearing soft tissue and ended with microsparitic to sparitic calcite in a microcrystalline groundmass comprising these fabrics; and (ii) if spongin components are present in fossils, why are they not visible along with spicule remains in spiculate demosponges in at least some cases (cf. Fig. 2A and B)?

## Layered fabrics

In Triassic stromatolites regarded by Szulc (1997) as containing sponges (Figs 6 to 9), the structure forms faint to prominent micrite layers containing porous network fabrics. Luo & Reitner (2014) used material from the same horizons; differences between images presented in Figs 6 to 9 and in Luo & Reitner (2014) demonstrate the variability of these microstructures. Layers in these materials broadly match the concept of spongiostromates, introduced by Gürich (1906) to convey their open architecture and layered bioaccretionary character (Figs 8 and 9). The spongiostromate microstructure is a microporous fabric of likely microbiotic accretion, generally blurred, grumelous (i.e. broadly clotted, see Bathurst, 1975, p. 511) to peloidal, at best faintly tubular to cellular/vesicular. This is in opposition to porostromate microstructures that display well-defined micro-organismic outlines preserved in growth position (Monty, 1981; for comparison, see Turner et al., 2000; Flügel, 2004, p. 122). In this context, layers comprise micrite normally enclosing somewhat irregular areas of sparite (Figs 8 and 9), although some have open pores and others with micrite in the pores (for example, Fig. 6F); the micrite may

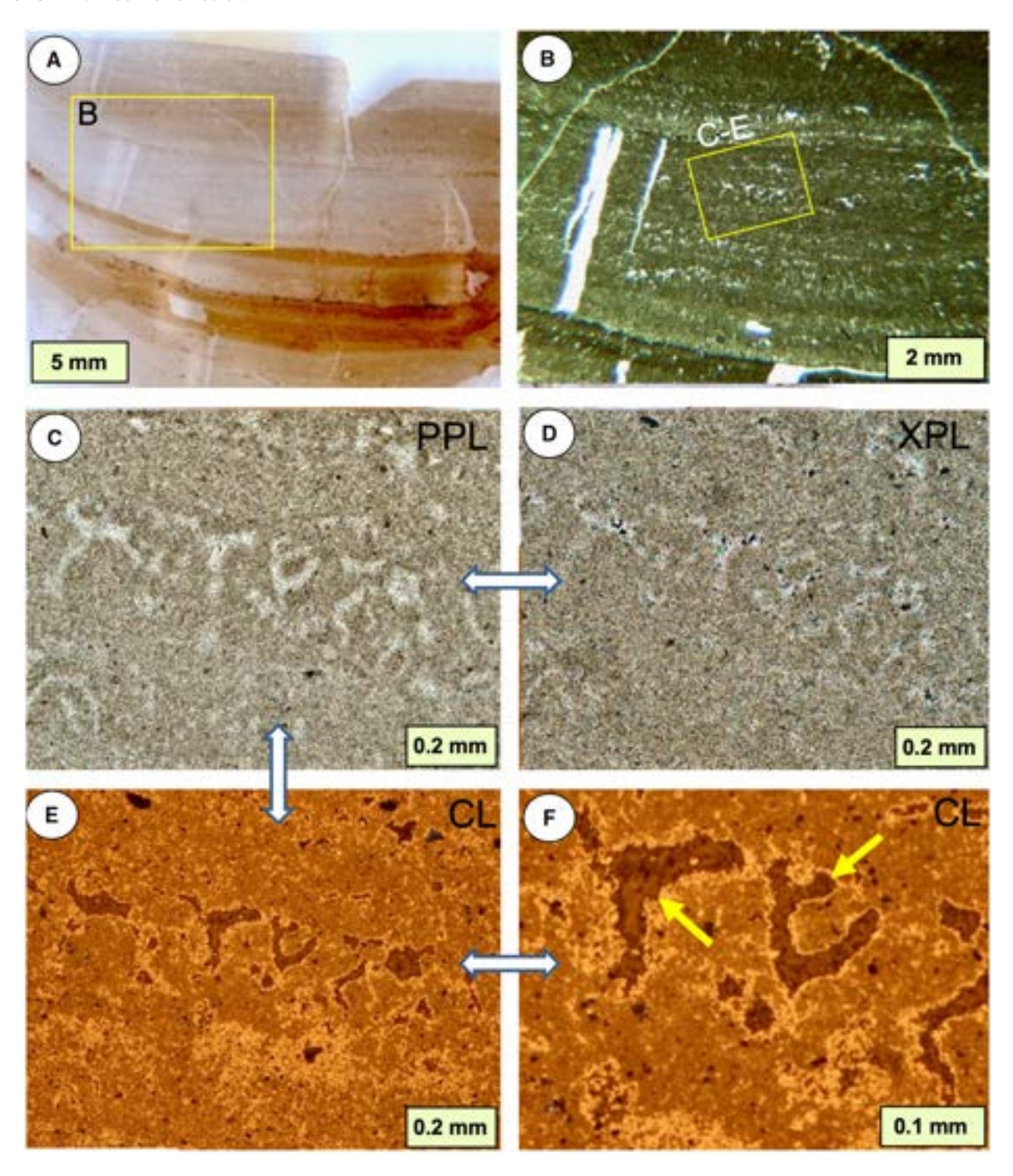


Fig. 8. Vertical thin sections from a Triassic stromatolitic horizon, containing vermicular structures. (A) and (B) General views of prominent layered structure and locations of (C) to (E). (C) and (D) plane-polarized light (PPL) (C) and cross-polarized light (XPL) (D) views of vermicular structure within stromatolite layers, showing sparite cement in the light areas. (E) and (F) Cathodoluminescence view of (C) and (D), with enlargement in (F), showing sequence of dull to no luminescence in sparite areas (arrow), while micrite areas contain a mixture of bright and dull luminescence. Note that edges of the micrite against sparite show a higher degree of brighter luminescence. This pattern is interpreted to indicate that sparite areas were vacated and infilled with cements, thus showing difference in diagenetic history from the micrite. From collections of Joachim Szulc, sampled by him from the Ladinian (late Middle Triassic), Negev area, Israel.

also include small bioclasts. Spongiostromate structures present a problem of interpretation because they have a spongy-looking fabric, in the common-English understanding of the term sponge, but without indication of a biological sponge nature, noting that Gürich's (1906) work did not infer sponges. However, Lee & Riding (2022) interpreted one spongiostromate fabric as a keratose sponge. The oldest known spongiostromate structures, forming part of oncoids, are Palaeoproterozoic (Schaefer et al., 2001; Gutzmer et al.. 2002). Examples spongiostromate-style fabrics interpreted to be keratose sponges may be seen in Luo & Reitner (2014, 2016), Pei et al. (2021a,b) and Lee & Riding (2021a,b, 2022). The present study includes Cambrian Cryptozoön samples (Fig. 10), that also show a spongiostromate character. Stock & Sandberg (2019) interpreted layered fabrics of spongiostromate form as sponges, in Devonian-Carboniferous boundary facies in Utah, but their photographs are insufficiently detailed to show structure clearly.

Layered fabrics may also show characters of fenestral-bird's eye fabrics, normally occurring in intertidal carbonate facies where degassing occurs in sediments exposed at the surface or in very shallow water (e.g. Tucker & Wright, 1990). They represent fabric-selective primary porosities with original voids commonly larger than the mean grain diameter. Sizes of pores in these fabrics are normally considered to be 1 to 3 mm, but network structures interpreted as keratose sponges are not larger than 0.1 mm (Luo & Reitner, 2014), so there is an apparent scale difference. However, Figs 6C, 6D and 7 show ranges of cavity sizes within the same layers, ranging from 0.1 to 3.0 mm. Those images are interpreted here to indicate that such porous layered fabrics may be small enough to overlap with the sizes of interpreted keratose sponge networks. Thus, laminae and sheets containing fabrics that may be reasonably described as fenestral, in Triassic (Anisian) microbialites/stromatolites, were considered to be keratose sponges by Luo & Reitner (2014, 2016). In a subsequent step, the interwas developed to propose pretation distinction between a stromatolite and a spongemicrobial 'consortium' called keratolite by Lee & Riding (2021a). Conventionally, such structures are understood to form via the entrapment of gas bubbles, anhydrite precipitation and desiccation, frequently in combination with dissolution and subsequent compaction in supratidal to intertidal (microbial) environments (Shinn,

1968). More recently, Bourillot *et al.* (2020) provided more details and a number of distinguishing parameters indicating that these porous microbialites/stromatolites may form laminated—micritic to laminated—peloidal microfabrics.

Layered fabrics shown in Figs 8 and 9 compare plane light views with CL in paired images; CL views show cement stratigraphy in the sparite, indicating void filling by a sequence of cement precipitation. CL views show variation in cement history, with bright and dull luminescent cements occurring at different stages. Commonly, bright cement is interpreted as early burial lowoxygen conditions where bacterial sulphate reduction (BSR) removes iron from porewaters, precipitated as pyrite, so that manganese causes bright luminescence; later, below the BSR zone, iron is added to quench the CL resulting in dull images (Scoffin, 1987). This sequence can be envisaged in Fig. 8F, although Fig. 9 shows a different sequence. Whatever the explanation of cementation history, it is difficult to visualize such structures as having resulted from permineralization of sponge tissues because they are composed of pore-filling cement.

#### **Network fabrics**

Networks comprise narrow areas of sparite surrounded by micrite as two broad types: (i) rectilinear networks of mostly criss-crossing straight lines of sparite with nodes (Figs 3G and H, 5A to D), reasonably interpreted as spiculate sponges; and (ii) curved networks of uncertain origin comprising convoluted areas of sparite vary from having equal thickness and sinusoidal form/shape to being more irregular. Both network types in thin section presumably exist as a three-dimensional (3D) network (e.g. Luo & Reitner, 2014, their 3D reconstruction). Rectilinear and curved networks in some cases resemble opaline spicule networks known from wellpreserved Palaeozoic heteroscleromorph sponges with rigid skeleton (lithistids; Fig. 5A to D and possibly Fig. 11A to D). Curved networks are illustrated in Neoproterozoic (Fig. 13E and F, reproduced from Turner, 2021), Cambrian and Ordovician facies (for example, Fig. 4C, reproduced from Lee & Riding, 2021a; see also Lee & Hong, 2019) and Permian-Triassic boundary microbialites (Brayard et al., 2011; Friesenbichler et al., 2018; Baud et al., 2021; Wu et al., 2021). Network fabrics in micrite inside articulated shells, embedded in micritic matrix lacking the networks, were interpreted by Park et al.

13653991, 2023, 3, Dowloaded from https://onlinelibrary.wiley.com/doi/10.1111/sed.1399 by Mount Holyoke College Library, Wiley Online Library on [02/01/2024]. See the Terms and Conditions (https://onlinelibrary.wiley.com/terms-and-conditions) on Wiley Online Library for rules of use; OA articles are governed by the applicable Cereative Commons. Licensecuted to the terms and Conditions (https://onlinelibrary.wiley.com/terms-and-conditions) on Wiley Online Library for rules of use; OA articles are governed by the applicable Cereative Commons. Licensecuted to the terms and Conditions (https://onlinelibrary.wiley.com/terms-and-conditions) on Wiley Online Library for rules of use; OA articles are governed by the applicable Cereative Commons. Licensecuted to the terms and Conditions (https://onlinelibrary.wiley.com/terms-and-conditions) on Wiley Online Library for rules of use; OA articles are governed by the applicable Cereative Commons. Licensecuted to the terms and Conditions (https://onlinelibrary.wiley.com/terms-and-conditions) on Wiley Online Library for rules of use; OA articles are governed by the applicable Cereative Commons. Licensecuted to the terms and Conditions (https://onlinelibrary.wiley.com/terms-and-conditions) on Wiley Online Library for rules of use; OA articles are governed by the applicable Cereative Commons. Licensecuted to the terms and conditions are governed by the applicable Cereative Commons.

3653919, 2023, 3, Downloaded from https://onlinelibrary.wiley.com/doi/10.1111/sed.13059 by Mount Holyoke College Library, Wiley Online Library on [02/01/2024]. See the Terms and Conditions (https://onlinelibrary.wiley.com/emers-and-conditions) on Wiley Online Library or rules of use; OA articles are governed by the applicable Creative Commons License

Fig. 9. Vertical and transverse sections from a Triassic stromatolitic horizon, containing vermicular structures. (A) and (B) plane-polarized light (PPL) (A) and cathodoluminescence (CL) (B) views of prominent vermicular structure in stromatolite. (C) and (D) Detail of structure from an adjacent area of thin section to (A) and (B). (E) Detail of another area of this sample at greater enlargement. (F) and (H) Transverse sections in PPL (F) and (G) and CL (H), demonstrating difference from vertical section views in (A) to (E), so the structure is not uniform in three dimensions. Images in this figure demonstrate differences in CL response between sparite and micrite areas, indicating their diagenetic histories do not coincide. From collections of Joachim Szulc, sampled by him from the Ladinian (late Middle Triassic), Negev area, Israel.

(2017, fig. 3) as spicule networks. Figure 12 shows examples of curved networks and microbial structures within microbialites directly after the end-Permian extinction; Fig. 12F shows two stages of micritic structure in those microbialites that are altogether incompatible with a sponge interpretation. Figures 13A to D and 14 explore more variations in Triassic curved networks using both plane light and CL, showing the variation in diagenetic history between the sparite areas and micrite areas. In particular, curved networks may grade into peloidal and amalgamated fabrics described below. Whether the presence of a clear boundary (for example, Fig. 18) defining network margins is an indicator that these structures are sponges or not, is considered in the Discussion.

## **Amalgamated fabrics**

Amalgamated structures comprise patches of micrite, which in some cases show vague individuality merged together with intervening spaces occupied by sparite (Fig. 9, which also shows layers, visible in Fig. 9A and B; see also Fig. 16A); samples viewed with CL in Fig. 9 show different cements in the sparite areas compared with the micritic areas, thus indicating voids filled with cement. They overlap with the concept of clotted micrites, but clotting implies a process of sedimentary material sticking together, which may or may not be appropriate, so are called amalgamated here. It is also possible that clotted fabrics may result from diagenetic change. Amalgamated fabrics have been described as keratose sponges by Lee et al. (2014) and Park et al. (2017, fig. 3), and discussed by Kershaw et al. (2021a) in comparison with possible sponges.

## **Granular fabrics**

These comprise dark-coloured micritic objects with irregular areas of light-coloured cement in spaces between objects (Fig. 15). The former may be peloids and commonly occur in cavities forming geopetals (Fig. 16, but compare with Figs 17, 19 and 20 considered in the Discussion). In many cases similar to Figs 16A and 17A to C attributed by authors to keratose sponges (e.g. Park et al., 2017, fig. 3E, F; Lee & Hong, 2019, fig. 2), granular fabric grades downward into amalgamated fabric, indicating fabric evolution from particulate to amalgamated downward with increased packing density. Because disaggregation of peloids into more diffuse masses of micrite is a common phenomenon, careful observation of intergranular and shelter porosity (thickness variation, grainsupported texture, sagging and dragging along pore walls) holds the key for discrimination of an essentially physical (abiotic) origin.

## Variegated spar fabrics

This is a separate category of sparite within micrite masses organized differently from the networks described above (Fig. 18). Variegated structures comprise an outer portion of short lines of sparite that curve round to form outer limits of a discrete structure, the inner portion is similar to network forms described above. Examples are in Luo & Reitner (2014, fig. 2f), Park et al. (2015, fig. 5D; 2017, fig. 5C), Friesenbichler et al. (2018, fig. 10B) and Lee et al. (2021, fig. 6D). Variegated structures seem to occur mostly in cryptic positions, although the case illustrated by Friesenbichler et al. (2018, fig. 10B) is in open space between microbialite branches.

#### DISCUSSION

In this study of a variety of shallow-marine carbonate microfabrics interpreted altogether as keratose sponges, four principal items need discussion: (i) verification of keratose sponge

13653991, 2023, 3, Dowloaded from https://onlinelibrary.wiley.com/doi/10.1111/sed.1399 by Mount Holyoke College Library, Wiley Online Library on [02/01/2024]. See the Terms and Conditions (https://onlinelibrary.wiley.com/terms-and-conditions) on Wiley Online Library for rules of use; OA articles are governed by the applicable Cereative Commons. Licensecuted to the terms and Conditions (https://onlinelibrary.wiley.com/terms-and-conditions) on Wiley Online Library for rules of use; OA articles are governed by the applicable Cereative Commons. Licensecuted to the terms and Conditions (https://onlinelibrary.wiley.com/terms-and-conditions) on Wiley Online Library for rules of use; OA articles are governed by the applicable Cereative Commons. Licensecuted to the terms and Conditions (https://onlinelibrary.wiley.com/terms-and-conditions) on Wiley Online Library for rules of use; OA articles are governed by the applicable Cereative Commons. Licensecuted to the terms and Conditions (https://onlinelibrary.wiley.com/terms-and-conditions) on Wiley Online Library for rules of use; OA articles are governed by the applicable Cereative Commons. Licensecuted to the terms and Conditions (https://onlinelibrary.wiley.com/terms-and-conditions) on Wiley Online Library for rules of use; OA articles are governed by the applicable Cereative Commons. Licensecuted to the terms and conditions are governed by the applicable Cereative Commons.

Fig. 10. Cryptozoön stromatolites of Lester Park Saratoga Springs, Hoyt Limestone, late Cambrian, New York (Goldring, 1938). (A) Field view of transverse sections of Cryptozoön from Lester Park, showing concentric laminae indicating domal form; lens cap 52 mm diameter. Photograph taken by Lisa Amati. (B) Hand specimen vertical section of Cryptozoön showing hemispheroidal to cabbage-like accretion; details of layering shown in (C) to (G). (C) to (G) Thin section views of variation of Cryptozoön proliferum Hall (hypotype, Goldring, 1938). Microfabrics in different layers of Cryptozoön structure including pelletoidal—cement—microspar (C), vertical—filamentous (D), and variations in vermiform structure (E) to (G). Microspar represents a replacement locally preserving some ghost structures of its host protruding upward (E) and (F); cement-filled sheet crack shown partly in the centre of (G). The nature of biolamination is illustrated in alternation of porostromate intervals [vertically oriented filaments (D)] with sets of spongiostromate texture. (A) NYSM\_E 1527; (B) Unregistered hand specimen in New York State Museum (NYSM); (C) and (F) NYSM-6503; (D), (E) and (G) NYSM-6505. Friedman (2000) emphasized that the structure of Cryptozoön comprises alternating layers of calcite and dolomite, but in a preliminary X-ray diffraction (XRD) test, in Laval University, of NYSM-6503 illustrated in (C) and (F) showed only calcite present.

affinity; (ii) alternatives to sponges; (iii) potential pitfalls of reporting; and (iv) the impact on understanding of ancient ecosystems. One prominent difficulty in assessing published illustrations is the low resolution of images, and common use of microscope sections that are thicker than normal and thus lack clarity.

### Verification of keratose sponge affinity

The wide variety of fabrics attributed to keratose sponges in the ancient record suffers from lack of verification, and in an early Neoproterozoic example (Turner, 2021; Fig. 13E and F), the age significantly pre-dates the expected appearance of its parent taxon, namely spongin-bearing demosponges (Fig. 2E). In Turner's (2021) study no mesoscopic body fossil with its overall shape and organization (architecture) that might help to determine its nature, is reported; and at the microscopic scale, there is a problem because no sponge-specific attribute such as the canal system (Aragonés Suarez & Leys, 2022) is preserved, although the enclosing microcrystalline phase is interpreted to represent automicrite resulting from mummification (Luo & Reitner, 2014, 2016). However, automicrite is not normally seen in published interpretations of keratose sponges (for examples, see Figs 4C, 13E and 13F). Thus, the preservation of the purported spongin skeleton requires understanding of a diagenetic pathway that seems to have no equivalent in the rock record.

Overall, claims for fossil keratose sponges in ancient carbonates require both proper identification of sponge structure and an exceptional preservation mechanism. Indeed, relatively decay-resistant structural tissue components such as parts of the extracellular collagenous matrix (ECM), mesoscopic strands and networks of spongin, the various forms of chitin  $(\alpha, \beta, \gamma)$ and cellulose might get physically preserved or mimicked via permineralization or via (geo-) polymerization (Gupta & Briggs, 2011). For the claim of keratose sponges in carbonates, permineralization (mummy-style preservation or spongin calcification) is considered a prerequisite in order to eventually preserve in 3D a largely uncompressed mesoscopic network of interpreted former spongin. Otherwise, if only the spongin skeleton is polymerized, the result should be severe physical compaction only episodically preserving exceptional details, as in Burgess-style preservation of sponges with tissue-related residues of organic carbon and in some cases pyrite (Conway Morris & Whittington, 1985; Butterfield & Nicholas, 1996; Ehrlich et al., 2013; Yang et al., 2017; Fan et al., 2021; Botting et al., 2022). The issue of canals in possible keratose sponges was addressed by Luo et al. (2022, fig. 5), with potential canals revealed through serial grinding, but more complete investigation is needed to prove that these structures are canals (see Table 1).

Sponge mummies, indirect representation of a former spongin skeleton

For a keratose sponge to permineralize in mummy-style, a body fossil should be produced that mimics (at least in part) exceptional details of the former organism *via* precipitation of microcrystalline carbonate (automicrite) at or near the sea-floor. Froget (1976, on lithistids) followed by Brachert *et al.* (1987, on hexactinellids) provided examples of Pleistocene to Holocene permineralized (calcified) siliceous sponges. In addition, these authors observed in some detail the concurrent onset of diagenetic

946 F. Neuweiler et al.

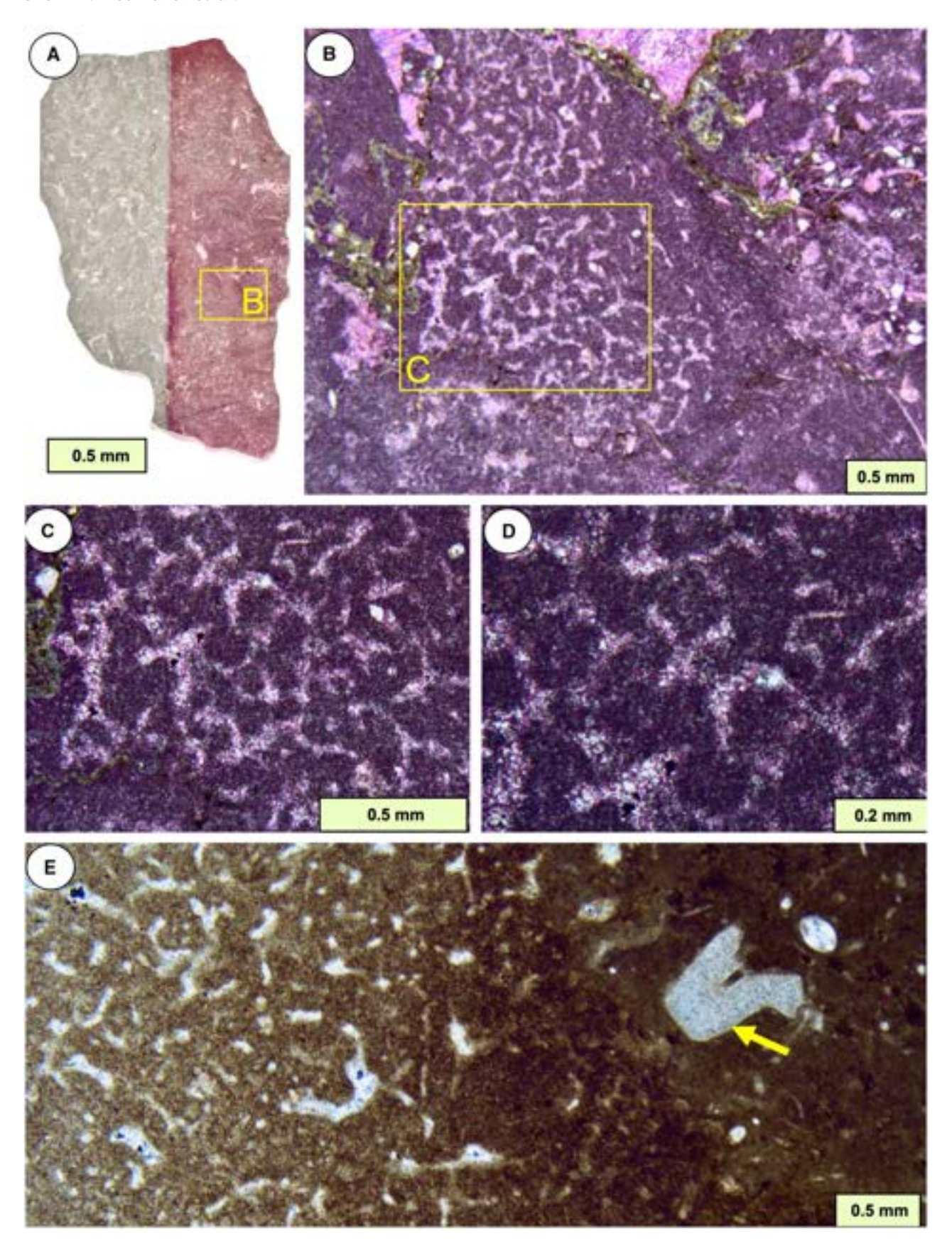


Fig. 11. (A) to (D) Vertical sections of matrix between stromatolite columns (not shown), containing a fragment of a possible keratose sponge in matrix, although this is instead possibly a lithistid. (A) Whole thin section partly stained with ARS-KFeCN, showing mottled fabric and location of (B). (B) The possible sponge forms a defined patch and shows curved network of sparite-filled voids embedded in micrite. (C) and (D) Details of (B) (D is a detail of the centre of C) showing sparitic nature of the network preserved as red-stained (non-ferroan) calcite. (A) to (D) from Chalk Knolls, Notch Peak Formation, upper Cambrian, Utah. (E) Curved network of sparite in micrite, but with a diffuse margin; a crinoid columnal (arrow) prominent in right hand part, outside the network. The network area may be a sponge, but its diffuse margin presents a problem of interpretation (Kershaw et al., 2021a). Huashitou reef, Ningqiang Formation, Telychian (lower Silurian), Guangyuan, northern Sichuan, China; specimen donated by Yue Li.

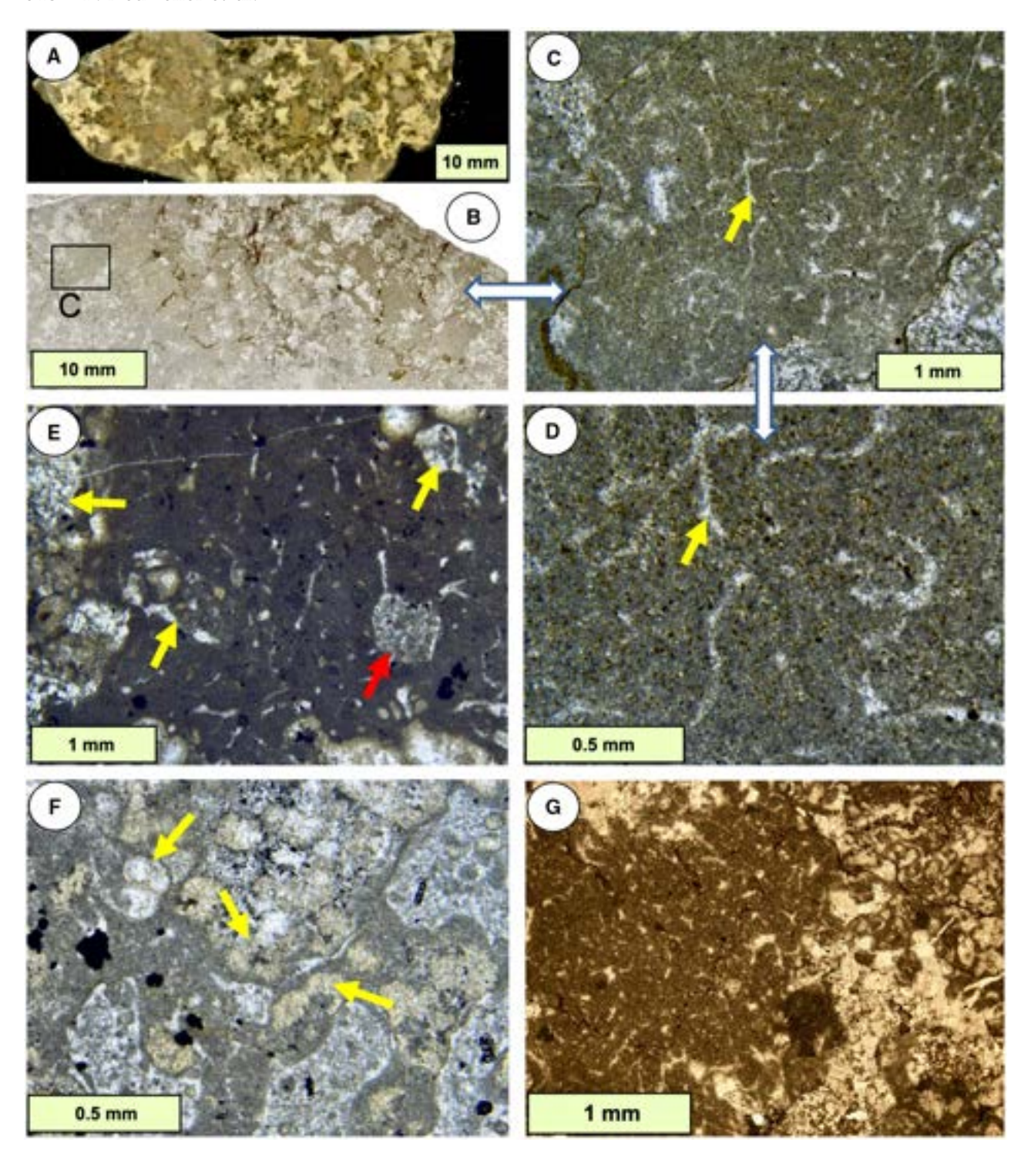
alteration of the opaline spicules (dissolution, initial cementation). Reitner (1993, p. 26 and Pl. 4/4) illustrated how a living non-rigid demosponge might preserve its original spicular architecture within automicrite. Neuweiler et al. (2007) observed an intimate connection of mummification with calcifying organic colloids adsorbed onto and into relatively decay-resistant parts of a former ECM during partial death corroborated by sponge bleaching. This involves dismantling and dissolution of fibrillar to amorphous collagenous matter in association with exudates of freshly-produced fluorescent dissolved organic matter (FDOM; Neuweiler & Burdige, 2005). In the Neuweiler et al. (2007) model, the dismantling of fibrillar collagen produces a nanoporous scaffold for calcification in of surface area, sorption capillarity-driven uptake of mineralizing fluids. Whatever the details are, mummified sponges represent distinct body fossils with well-defined outer boundaries towards their enclosing sediment, presumably mirroring the physical specifics of an encountered sponge ectosomal tissue.

Permineralizing modern sponges, except for being a curiosity, typically are very rich in fibrillar collagen giving them a firm-leathery (for example, the spiculate Spheciospongia, Wiedenmayer, 1978) to even cartilaginous consistency (for example, the reportedly petrifying verongimorph Chondrosia, Göthel, 1992). Nevertheless, it remains questionable whether this small group of extant sponges is representative of fossil sponge mummies (Neuweiler et al., 2007, for short review). For a number of sponge mummies, there is a problem of sheer volume, that is the amount of ECM (extracellular collagenous matrix) present in modern sponges does not necessarily match the larger amount of automicrite observed. Malumispongium (Bourque & Gignac, 1983; Neuweiler et al., 2007) might serve as an extreme example (Fig. 3A to E). Therefore,

unresolved microbial-organochemical reactions might be involved, and even dissolved porewater silica might play a role if opaline spicules were originally abundant (Lakshtanov & Stipp, 2010).

Overall, if the fine-grained portions of any microfabric proposed to represent an indirect model of a former mesoscopic spongin skeleton was preserved via mummification, then its transformation must have produced a distinct body fossil within an already consolidated to indurated structure, simply to prevent compression of a highly elastic organic skeleton (see Jesionowski et al., 2018, fig. 10). The light-coloured network structures illustrated in Luo & Reitner (2014, 2016), Lee & Riding (2021a,b) and Turner (2021), in concert with the results herein, do not show compression. This might be the reason why the keratose sponge interpretation calls for the presence of automicrite via mummification (Luo & Reitner, 2014, 2016), but there is no supporting petrographic or geochemical evidence for automicrite in those published cases. Such evidence might include: gravity-defying, secondary (stromatactoid) voids, fragmentation, local collapse, extractable fluorescence, intracrystalline organic compounds of low molecular weight, and eventually specific rare earth element (REE-) patterns indicating the role of natural organic matter (NOM; see Pourret et al., 2007); altogether pointing to natural humification processes acting in concert with the formation of sponge-related automicrite (Neuweiler et al., 1999, 2000, 2001, 2003, 2007, 2009; see also James & Jones, 2015, p. 28).

Discrete preservation of a spongin skeleton Because spongin that forms the mesoscopic skeleton of keratose sponges is a non-fibrillar collagen (Garrone, 1978; Exposito et al., 1991), during decay, no dismantling and respective sorptive attributes (aspects of mummification)



are expected to occur. Thus, the mesoscopic spongin skeleton appears not prone to permineralize. This issue appears significant because claims for fossil keratose sponges involve statements that spongin was replaced by calcite or

calcified (Reitner *et al.*, 2001). Another option is mineral coating, that is mineral precipitation and growth at and from the spongin surface, but there are no cases reported for the rock record, and little information comes from modern

Fig. 12. Examples of curved network fabrics in Permian-Triassic boundary microbialites from south China. (A) hand specimen and (B) thin section of microbialite a few centimetres above the end-Permian mass extinction horizon, showing recrystallized microbial calcite (lobate pale areas in B) with intervening micrite. (C) and (D) Enlargements of box in (B) showing curved, distinct to diffuse sparitic areas (arrow) in the micrite (containing abundant microdolomite), similar material to that interpreted as keratose sponge by Baud et al. (2021) and Wu et al. (2021). Permian-Triassic boundary interval, Baizhuyuan site, Huaying Mountains, Sichuan, China. (E) Another sample of microbialite after end-Permian extinction, with curved sparite patches as in (A) to (D), but in this case the sparite may be recrystallized bioclasts. This image also shows lobate areas of light-coloured sparite (yellow arrows), that are the calcimicrobe frame which constructed the microbialite (Kershaw et al., 2021b). Red arrow indicates a patch of fine-grained peloidal fill in an interpreted cavity in the darker micrite fill. (F) A transverse section of microbialite showing the calcimicrobial frame (yellow arrows) and two generations of fill; generation 1 (darker grey) contains elongate sparite patches similar to vermiform fabric in (D); generation 2 is a fine-grained peloidal infill. (E) and (F) from Laolongdong site, Beibei, Chongqing, China. (G) Right-hand third shows partially altered calcimicrobial structure, comparable to that described by Ezaki et al. (2008, fig. 8C, from the Dongwan locality a few kilometres along strike from A-D) as 'spongelike'. Left-hand two thirds show micrite infill, containing network fabrics, deposited between microbial branches. See text for discussion.

keratose sponges (see Towe & Rützler, 1968, who described iron oxide granules embedded in spongin). Szatkowski et al. (2018), working in the field of biomimetics (the branch of science that explores use of natural materials to solve human problems) showed that it is possible to experimentally coat spongin fibres with mineral (in their case it was MnO<sub>2</sub>). The Szatkowski et al. (2018) study is a parallel to the idea that. in carbonate environments, spongin of keratose sponges may be useable as a substrate for mineral overgrowth, that might preserve the shape of the spongin network in diagenesis. In carbonates, if the network represents a sponge, then the spongin network is represented as calcite, but it would not be possible to know whether this is due to calcification of the spongin structure (a process that has not been demonstrated diagenetically) or is due to cement infilling of the mouldic space left when the spongin protein decayed. The key point is that there is no evidence of mineral overgrowth in structures of possible keratose sponges; thus it is not currently possible to determine if mineral overgrowth could preserve the form of the spongin skeleton.

Cathodoluminescence images presented in Figs 8, 9 and 13 to 15 largely show that sparite areas have different cements from the micrite; in some cases (for example, Figs 8F, 9 and 14) there are zoned cements in sparite that indicate early porosity and permeability, so this seems to preclude any mineralization process related to the spongin itself, at least for these samples. Even in Fig. 13A to D, where the distinction between the micrite and sparite areas in CL is minimal, parts of the sparite show different CL

response from the micrite. Thus, in the cases illustrated in this paper, there is no obvious basis for any kind of mineralization of the spongin itself to explain the sparitic areas. It is easier to attribute CL responses to early cementation of porosity; this does not necessarily deny a sponge affinity in other cases but would leave mummification as the only option left to explain preservation of keratose sponges in carbonate rocks. However, as explained earlier, for this option, there is no supporting petrographic-geochemical evidence. Last, but not least, abundant modern demosponges containing opaline spicules attached to prominent strands of spongin (Axinellidae, Fig. 2A and B) should, as fossils, show both spar-cemented spicule moulds together with their associated moulds of spongin. No published report of such an intimate relationship preserved in carbonate rock thinsection was found in the literature or in any material studied during this investigation.

A significant issue is recognition of a canal system specific to sponges (Figs 1A, 1B, 2C, 2D, 3 and 4). If sponge mummies are present, a canal system with cortical distinction might be preserved in detail even in the absence of a spicular skeleton (Fig. 3A to E; Bourque & Gignac, 1983; Neuweiler et al., 2007, fig. 1A, B). Recently, Aragonés Suarez & Leys (2022) proposed a model for fossil sponge recognition based on the presence of a canal system. However, there are no verified canals in all the fossil examples illustrated here and in publications interpreting keratose sponges examined in this study. Neuweiler et al. (2009) denied the presence of sponges in early Neoproterozoic polymuds because of the lack of any signs of a

13653991, 2023, 3, Dowloaded from https://onlinelibrary.wiley.com/doi/10.1111/sed.1399 by Mount Holyoke College Library, Wiley Online Library on [02/01/2024]. See the Terms and Conditions (https://onlinelibrary.wiley.com/terms-and-conditions) on Wiley Online Library for rules of use; OA articles are governed by the applicable Cereative Commons. Licensecuted to the terms and Conditions (https://onlinelibrary.wiley.com/terms-and-conditions) on Wiley Online Library for rules of use; OA articles are governed by the applicable Cereative Commons. Licensecuted to the terms and Conditions (https://onlinelibrary.wiley.com/terms-and-conditions) on Wiley Online Library for rules of use; OA articles are governed by the applicable Cereative Commons. Licensecuted to the terms and Conditions (https://onlinelibrary.wiley.com/terms-and-conditions) on Wiley Online Library for rules of use; OA articles are governed by the applicable Cereative Commons. Licensecuted to the terms and Conditions (https://onlinelibrary.wiley.com/terms-and-conditions) on Wiley Online Library for rules of use; OA articles are governed by the applicable Cereative Commons. Licensecuted to the terms and Conditions (https://onlinelibrary.wiley.com/terms-and-conditions) on Wiley Online Library for rules of use; OA articles are governed by the applicable Cereative Commons. Licensecuted to the terms and conditions are governed by the applicable Cereative Commons.

Fig. 13. (A) to (D) Vertical sections of vermicular structure in plane-polarized light (PPL) and cathodoluminescence (CL) views. (A) light branched and curved areas are sparite embedded in micrite. (B) CL view of same area as (A). (C) and (D) Enlargements of (A) and (B), respectively; arrows show matched points in the four photographs. CL view (B) and (D) shows little difference in CL pattern between the two components; sparite contains poorly luminescent and bright luminescent areas, and micrite shows a similar variation at a smaller scale, in fine-grained material, giving it a speckled appearance. Some sparite in PPL is indistinguishable from micrite in CL. Whether this uniform CL response supports or denies a keratose sponge origin of this vermicular structure is open to discussion. From boundary between *Diplora* Beds and overlying Tarnowice Beds, Muschelkalk, Middle Triassic, Libiaż Quarry, Upper Silesia, Poland. (E) and (F) Vermicular structure from Neoproterozoic carbonates described by Turner (2021, Extended data fig. 1B and C). Note sparite-filled network fabric. Reproduced under Creative Commons licence (http://creativecommons.org/licenses/by/4.0/), with acknowledgment to *Nature*.

preserved canal system. On the other hand, the canal system (together with spicules) might be too tiny to be visually preserved, although other observations (automicrite, context, substrate) may indicate a sponge interpretation (Shen & Neuweiler, 2018). Lee & Riding's (2021b) reconsideration of the enigmatic structure Cryptozoön provides an excellent example of the overall problem of sponge recognition; despite high quality preservation, there is no canal system and there is no cortical distinction (Fig. 10, and illustrations in Lee & Riding, 2021b). In thin sections circular or elliptical features in crosssection may be canals, but without 3D evidence, verification is not possible; for example, this issue affects the interpretation by Lee & Riding (2022) that the Mississippian Spongiostroma originally described by Gürich (1906) is a sponge. Evidence for the presence of keratose sponges [in opposition to conventional (microbial) spongiostromatal is needed to test the original interpretation (Luo & Reitner, 2014, 2016).

Another example of the problem of verification is shown in Heindel et al. (2018, figs 9D, 10B, 10D), in microbialites from the well-known Çürük Dag site in southern Turkey. Heindel et al. (2018) labelled sponges as being present in the matrix between microbial branches, but close examination of those images reveals a homogenous calcareous mudstone with minute bioclasts and cannot be considered a sponge mummy. Other images in the same paper show areas of matrix containing fine sparite between microbial branches that may be networks, but lack criteria proving they are sponge mummies; a similar example from south China was discussed in detail by Kershaw et al. (2021a).

In summary, because they lack verification, the presence of fossil keratose sponges in thinsections made from limestones—dolostones is called into question. Table S1 represents an

effort to requalify the most prominent examples as: essentially microbial-related (spongiostromate, bird's eyes—vugular—fenestral porosity), biogenic—problematic, and dubiofossil to even pseudofossil in nature.

# Alternatives to sponges

#### Endobenthos

Geopetal cavities of variable context including articulated shells frequently show an infilling deposit that grades downward from peloids into amalgamated micrite (for example, Figs 16 and 17A to C). Several are interpreted as sponges (Lee & Hong, 2019, fig. 2). However, in modern marine cavities similar fabrics are reported to form simply by compaction of settled grains (MacIntyre, 1978; Moore, 2001, fig. 5.11; James & Jones, 2015, fig. 24.6).

An alternative is that these fabrics reflect burrowing of cavity sediment by small organisms. Such small organisms generally fall within the definition of meiofauna (0.04 to 1.0 mm across), but some can be down to a few microns and up to 2 mm (see review of Löhr & Kennedy, 2015) so clearly matching the width of sparite areas in vermiform networks. Meiofauna is a broad group of benthic invertebrates that includes nematodes, foraminifera, annelids (particularly polychaetes) and arthropods (ostracodes, malacostracans; Giere, 2009; Traunspurger & Majdi, 2017). They are important contributors of modern sediments, reaching densities of up to 1500 individuals per 10 cm<sup>2</sup> (e.g. Shirayama & Kojima, 1994; Neira et al., 2001; Guilini et al., 2011), modifying sediment chemistry (summary of Schratzberger & Ingels, 2018) and producing dense networks of sinusoidal burrows (Cullen, 1973; Pike et al., 2001) or simply blurring the primary sediment fabric without even discrete traces (Pemberton et al., 2008), which was also shown by laboratory

Fig. 14. Vertical sections of Triassic vermicular structure in plane-polarized light (PPL) and cathodoluminescence (CL) views, for comparison with Figs 7, 8 and 12. (A) Light branched and curved areas are sparite embedded in micrite; (B) is the matched CL view. (C) and (D) Enlargements of (A) and (B), respectively; arrows show matched points in the four photographs. Although initial examination indicates differences from Figs 7, 8 and 12, CL patterns in these figures only show variable amounts of poor and bright luminescent areas in sparite, yet some areas of the sparite are also indistinguishable from micrite in CL view. From boundary between *Diplora* Beds and overlying Tarnowice Beds, Muschelkalk, Middle Triassic, Libiaż Quarry, Upper Silesia, Poland.

13653091, 2023, 3, Downloaded from https://onlinelibrary.wiley.com/doi/10.1111/sed.13059 by Mount Holyoke College Library, Wiley Online Library on [02/01/2024]. See the Terms

s-and-conditions) on Wiley Online Library for rules of use; OA articles are governed by the applicable Creative Commons License

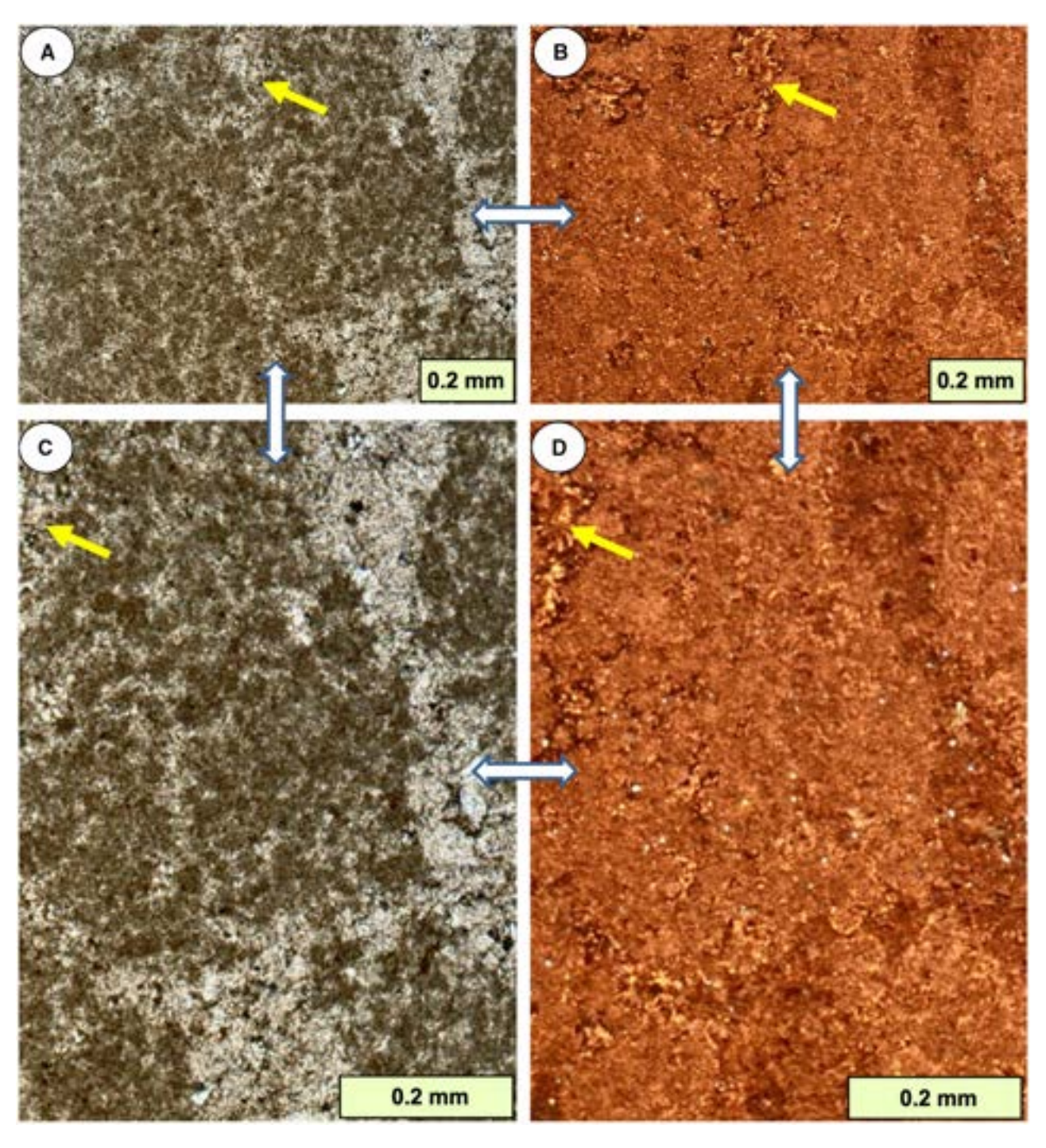


Fig. 15. Vertical sections of peloidal structures from Viséan limestones of Boulonnais inlier, northern France. (A) and (B) plane-polarized light (PPL) (A) and cathodoluminescence (CL) (B) views of peloidal carbonate, showing bright orange luminescence of peloids; and dull orange to yellow luminescence of interpeloidal calcite cement. (C) and (D) Details of the structure, arrows mark matched points. These images demonstrate that peloidal fabrics are not compatible with an evidence-based interpretation as sponges, and may instead be a diagenetically altered particulate carbonate or microbial deposit.

13653991, 2023, 3, Dowloaded from https://onlinelibrary.wiley.com/doi/10.1111/sed.1399 by Mount Holyoke College Library, Wiley Online Library on [02/01/2024]. See the Terms and Conditions (https://onlinelibrary.wiley.com/terms-and-conditions) on Wiley Online Library for rules of use; OA articles are governed by the applicable Cereative Commons. Licensecuted to the terms and Conditions (https://onlinelibrary.wiley.com/terms-and-conditions) on Wiley Online Library for rules of use; OA articles are governed by the applicable Cereative Commons. Licensecuted to the terms and Conditions (https://onlinelibrary.wiley.com/terms-and-conditions) on Wiley Online Library for rules of use; OA articles are governed by the applicable Cereative Commons. Licensecuted to the terms and Conditions (https://onlinelibrary.wiley.com/terms-and-conditions) on Wiley Online Library for rules of use; OA articles are governed by the applicable Cereative Commons. Licensecuted to the terms and Conditions (https://onlinelibrary.wiley.com/terms-and-conditions) on Wiley Online Library for rules of use; OA articles are governed by the applicable Cereative Commons. Licensecuted to the terms and Conditions (https://onlinelibrary.wiley.com/terms-and-conditions) on Wiley Online Library for rules of use; OA articles are governed by the applicable Cereative Commons. Licensecuted to the terms and conditions are governed by the applicable Cereative Commons.

Fig. 16. Vertical sections through geopetal fabrics in early-formed cavities in shallow marine limestones, containing peloidal and clotted micrites. (A) Geopetal cavity in a mud-rich coral reef, shows variation from separate peloids at top, down to amalgamated fabrics in lower part, interpreted by Kershaw et al. (2021a) as either inorganic or microbially related structures, in contrast to interpretation of similar structures as keratose sponges. Huashitou reef, Ningqiang Formation, lower Silurian, Guangyuan, north Sichuan, China. Reproduced from Kershaw et al. (2021a), under CC-BY-NC 4.0, with acknowledgement to Yue Li, The Sedimentary Record and SEPM. (B) and (C) Geopetal cavity in an algal reef, with layered peloids interpreted as sedimentary, with possible microbial influence. Note that (B) is cross-polarized light (XPL) and the two black areas at top are holes in the thin section; (C) is in plane-polarized light (PPL). Late Quaternary, Aci Trezza, eastern Sicily, Italy; after Kershaw (2000). (D) and (E) Geopetal cavity in algal—coral reef with interpreted particulate peloids and cements. Both images are PPL; blue colour is resin-filled empty space in the geopetal. Holocene, Mavra Litharia, central south coast of Gulf of Corinth, Greece; after Kershaw et al. (2005).

experiments (Bonaglia et al., 2014; Schieber & Wilson, 2021). In the ancient record, the activity of meiofauna is under-represented because of the small size of the organisms and their burrows which cause: (i) tiny burrows that easily undergo compaction; (ii) no lithological difference between the burrow infill and surrounding sediment; and (iii) some in sand are smaller than the grain size (see summary of Schieber & Wilson, 2021). Consequently, recognition of meiofauna burrows in sedimentary rocks is in early development (see also McIlrov, 2022). In the small number of available publications (Knaust, 2007, 2010, 2021; Baliński et al., 2013; McMenamin, 2016; Parry et al., 2017; Villegas-Martin & Netto, 2018; Biddle et al., 2021), meiofauna burrows may be identified by their constant diameter and straight to sinusoidal character, with a producer being sometimes preserved at the end of the trace (Knaust, 2007, 2021). The traces generally have no ichnotaxonomic names, with only few exceptions that could be assigned to Cochlichnus, Trichichnus, Helminthopsis or Helminthoidichnites (Knaust, 2007; Villegas-Martin & Netto, 2018).

Features diagnostic of meiofauna tunnels (straight to sinusoidal shape, constant diameter) are seen in published photographs interpreted by some authors as keratose sponges (e.g. Park et al., 2015, fig. 8A). Moreover, some meiofauna burrows concentrate within macrofauna burrows and whole shells, most likely utilizing specific living conditions and scavenging on decaying tissues and bacteria (Villegas-Martin & Netto, 2018; Knaust, 2021). In this context, the features in Luo & Reitner (2014, fig. 2f) and Park et al. (2015, fig. 4D), reproduced in Fig. 18, are potential macrofaunal burrows penetrated by meiofauna, whereas Park et al. (2015, fig. 8B) presented a whole brachiopod shell that may have been passively filled with micrite and

subsequently penetrated by meiofauna produce vermicular-structured micrite. Figure 19 shows a Cambrian example of potential microburrow networks in a cavity, noting that the images also indicate geopetal sediment in the sparite areas indicating an open network prior to cementation. Figure 19E and F, using UV fluorescence microscopy shows in this monochrome image that brighter areas are outside the network, interpreted to indicate that the network is not composed of automicrite and thus not related to sponge mummification. The accompanying CL image (Fig. 19F) indicates brighter luminescence in the sediment that may reflect diagenetic alteration. Figure 20 shows a case of cavities inside the outer portion of a stromatolitic dome in shallow marine platform carbonates from North China; the cavities contain micrite and some type of network that does not resemble a sponge, and may be interpreted as a microburrow nest. Summarizing, the ubiquity of meiofaunal burrowing in modern environments and the similarity of some ancient network structures to those burrows provide a viable alternative to at least some of the possible keratose sponge interpretations.

# Dubiofossils to pseudofossils

Three-dimensional microcrystalline micronetworks might result from cementation of interparticle porosity of fine-grained granular—peloidal sediment material (Macintyre, 1985; Lokier & Al Junaibi, 2016; Kershaw et al., 2021a). The issue is complicated because the initial state and cohesiveness of peloidal material varies greatly from loose aggregates—floccules to indurated grains via an entire spectrum of plasticity (Schieber et al., 2013). The consequences might be severe because during consolidation and physical compaction the initial granular texture might be lost, resulting in a grumelous ghost

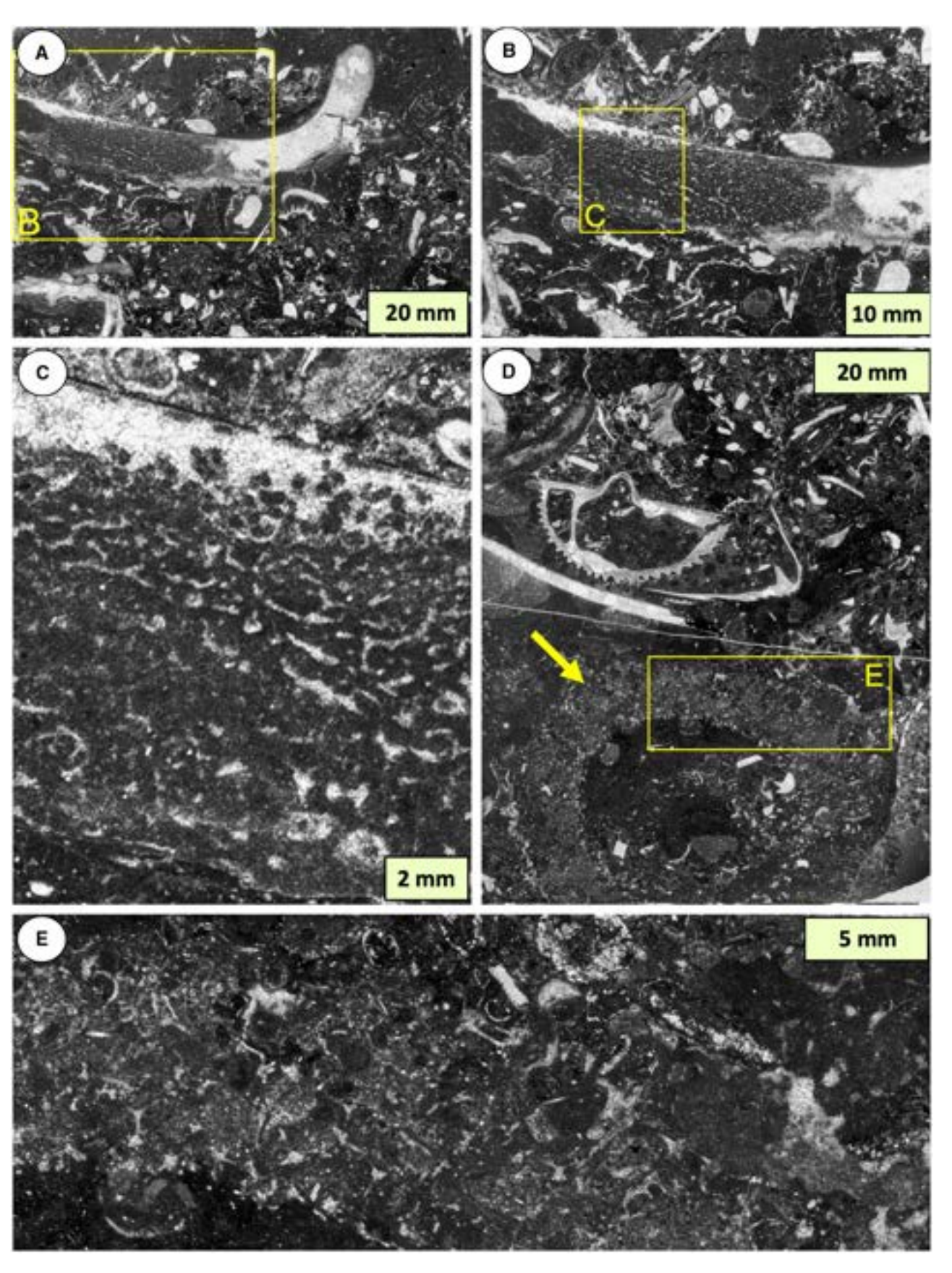


Fig. 17. Contrasting images of amalgamated and peloidal fabric (A) to (C), siliceous demosponges (D) and (E). Reef material in early Floian (Ordovician) carbonates, Huanghuachang Section, Hunghuayuan Formation Basin (GPS: N 30°51.541/E 111°22.713). (A) to (C) amalgamated to peloidal fabric that evolved as infiltrated sediment subsequent to aragonite dissolution within molluscan mouldic pore. The overall context implies a preservational window of earliest granular sediment textures (indurated and soft peloids, carbonate floccules, disaggregation) along with sediment consolidation under minimal mechanical compaction. (D, detail in E) Complexity of an Ordovician reef fabric. Well-preserved siliceous demosponge (yellow arrow), mummified whereby lighter automicrite preserves some darker spots of matrix sediment representing part of sponge canal system.

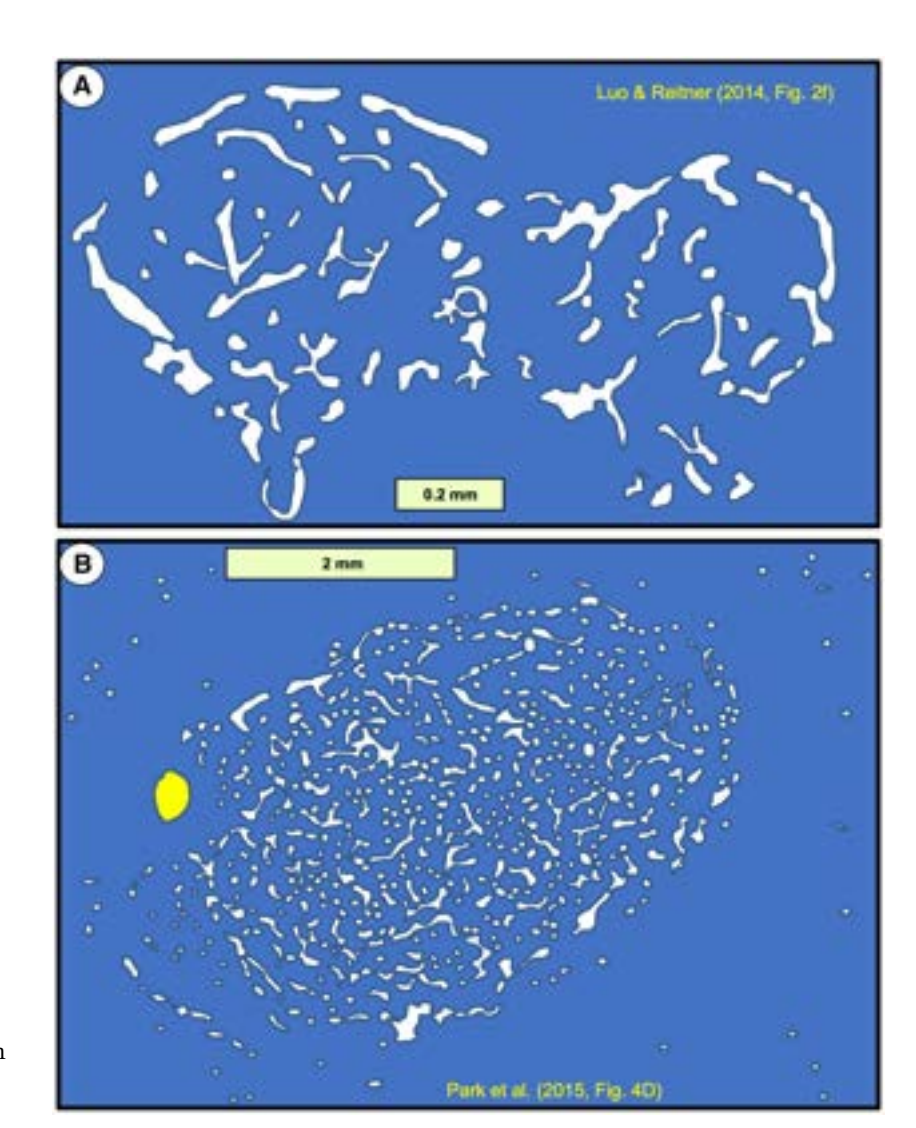


Fig. 18. Traced drawings of variegated fabrics, from (A) Luo & Reitner (2014) and (B) Park et al. (2015) to show pattern of sparite (white), with an outer broken border of curved areas of sparite. Blue background in each case is micrite, lacking any clotted or automicrite fabrics and is presumed to be sediment matrix. In (B) yellow ellipse is likely an ostracod shell.

structure or even a diagenetic mudstone texture (Lokier & Al Junaibi, 2016, for full discussion). Peloidal textures might also result from authigenesis (pelletoidal automicrite) and heterogenous aggrading neomorphism (Bathurst, 1975, p. 505, fig. 350; Dickson, 1978; Macintyre, 1985). The examples of peloidal textures in geopetal infills in cavities presented by Lee & Hong (2019) as

sponges can be alternatively interpreted as peloidal fills in cavities. In another example, the microspar groundmass in Turner's (2021) study of Neoproterozoic vermiform structure contains no features that would indicate that it originated through 'permineralization of a pre-existing biological substance' (Turner, 2021, p. 2), that is, automicrite. A vermiform microstructure in a

#### 958 F. Neuweiler et al.

**Table 1.** Tabulation of the six criteria for recognition of keratose sponges by Luo *et al.* (2022), with comments on their applicability. Source: Luo *et al.* (2022).

| No. | Luo <i>et al.</i> (2022) criteria for keratose sponges   | Comments (this study)  |
|-----|--|--|
| I   | "Fibrous skeletons are preserved as microspar-cemented moulds in homogeneous automicrites."  | As demonstrated in the main text, there are various possible explanations for such features, of which keratose sponge is one. Therefore, this criterion is not reliable for a keratose sponge interpretation. Note also that sponge-related automicrites are far from being homogenous, instead they generally form part of a void-complexing sequence with multiple infills.  |
| II  | "The skeletal fibres form an anastomosing network extending three-dimensionally in the micritic aggregation with a generally uniform density."   | Three-dimensional networks with uniform density do not have to be only sponges; for example, microburrow networks. Thus: (i) it would be necessary to demonstrate that the observed 'fibres' are skeletal in nature; and (ii) although this criterion is a theoretical possibility, it raises the question of why this has to be diagnostic for a sponge.  |
| III | "The skeleton persists a uniform thickness along each fibre. In the whole skeletal frame, the fibre thicknesses either change gradually or exhibit regular orders or hierarchies. For reference, the diameters of skeletal fibres in living nonspicular demosponges vary from a few to hundreds of micrometres, with many being around tens of micrometres thick (Figure 2; Supplementary File S2)." | (i) In contradiction to this criterion, Luo <i>et al.</i> (2022, fig. 2) shows that fibres vary in thickness, but the first sentence of this criterion says they are uniform (and the second sentence says they vary); therefore, the observations do not seem to be stabilized. (ii) Noting the variety of overlapping components in fig. 2, there is no reason why these networks have to be sponges. (iii) Perhaps a 3D network sectioned in 2D may show a large number of dots representing elements cut in transverse section; this expectation contrasts the branched networks commonly seem in thin sections, and so cases with such dots may be more reliably viewed as sponges. |
| IV  | "The fibrous network is constrained in<br>the micritic aggregation and exhibits<br>fibres lining the border of the<br>aggregation, such as between the<br>sponge body and the hard substrates<br>and wrapped particles."   | This is a reasonable criterion, a border to a sponge may be expected. It means that a substantial number of figured keratose sponges in recent years' papers are excluded. However: (i) the presence of a border does not exclude the possibility that the structure is something else; maybe it is the border of a burrow network; and (ii) it is also necessary to consider taphonomic and diagenetic processes that might modify the border lining, making the margin more diffuse. Thus, this criterion is not diagnostic for a sponge.  |
| V   | "There are no desmas (cf. Figure 1D), incorporated spicules, or orthogonal symmetry (Figure 1A,B) in the fibrous network that could indicate an affinity of spicular sponges."   | However, desmata would not be expected in a keratose sponge, so this is really an absence criterion and is therefore not diagnostic for a keratose sponge; there remains no confirmation that the structure is a sponge.   |
| VI  | "Water canals of the sponge aquiferous system are sometimes preserved (Figure 1E,F; more discussion in Section 4.1). If present, they add credits to the sponge interpretation."   | Much depends on their mesoscopic 3D structure; the so-called aquiferous canals illustrated in recent papers are just circular patches of sparite in thin section; thus, it remains unclear what shape and architecture they display if they could be envisaged in mesoscopic 3D.   |

sheltered void in Turner (2021, extended data, fig. 2) grades into the underlying and overlying homogenous microspar; the lack of a sharp contact between the vermiform area and adjacent micrite reduces confidence that this structure is a sponge (but see Table 1). The Early Neoproterozoic vermiform microstructure (Turner, 2021) may indeed be a dubiofossil or even a pseudofossil (syneresis). Furthermore, although

they have some resemblance to microburrow nests observed in Phanerozoic limestones (graphoglyptid trace fossils, see Kris & McMenamin, 2021), it seems unlikely that meiofaunal metazoans would have existed in the Early Neoproterozoic, so the respective claim for presence of a worm-like (bilateralian) organism (Kris & McMenamin, 2021) would even intensify the conflict with respect to current knowledge about

959

Keratose sponges in ancient carbonates

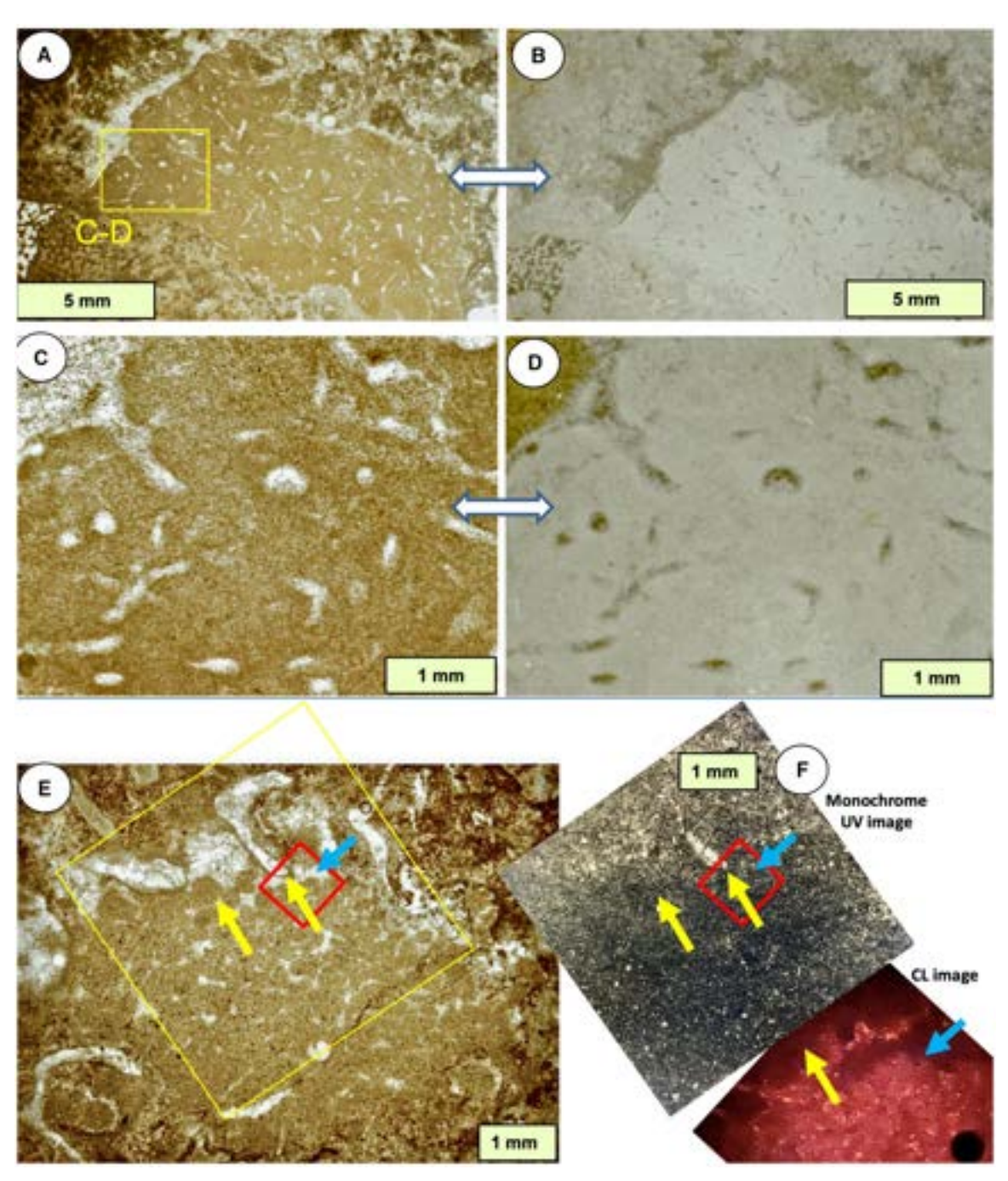


Fig. 19. Vertical sections through vermicular structures in cavities in Cambrian carbonates, interpreted by McMenamin (2016) as meiofaunal burrows (microburrow nest) rather than sponges. (A) and (B) plane-polarized light (PPL) (A) and reflected light (B) views of vermicular structures within a cavity in an archaocyath–algal bound-stone. Here, vermicular structures are interpreted as possible graphoglyptid trace fossils comprising microburrow swarms (McMenamin, 2016). (C) and (D) Details of box in (A), using PPL (C) and reflected light (D) views. Puerto Blanco Formation, Lower Cambrian, base of unit 3, Cerro Rajón, Sonora, México. (E) and (F) Vermicular structure in interior space of an archaeocyath, interpreted as packed faecal pellets in a cavity. (E) is PPL, (F) shows ultra violet (UV; upper image) and cathodoluminescence (CL; lower image); red box in UV image shows location of CL photograph; yellow and blue arrows show matched points between these three images. Pellets are discrete in upper part of cavity but become more diffuse downward, interpreted by McMenamin (2016) to indicate pellets disaggregated in lower part of the pile and light areas are interpreted as microburrows in sediment, burrowing activity may have caused disaggregation of pellets. Poleta Formation, Cambrian Stage 3, Barrel Springs, Nevada, after McMenamin (2016).

13653991, 2023, 3, Dowloaded from https://onlinelibrary.wiley.com/doi/10.1111/sed.1399 by Mount Holyoke College Library, Wiley Online Library on [02/01/2024]. See the Terms and Conditions (https://onlinelibrary.wiley.com/terms-and-conditions) on Wiley Online Library for rules of use; OA articles are governed by the applicable Cereative Commons. Licensecuted to the terms and Conditions (https://onlinelibrary.wiley.com/terms-and-conditions) on Wiley Online Library for rules of use; OA articles are governed by the applicable Cereative Commons. Licensecuted to the terms and Conditions (https://onlinelibrary.wiley.com/terms-and-conditions) on Wiley Online Library for rules of use; OA articles are governed by the applicable Cereative Commons. Licensecuted to the terms and Conditions (https://onlinelibrary.wiley.com/terms-and-conditions) on Wiley Online Library for rules of use; OA articles are governed by the applicable Cereative Commons. Licensecuted to the terms and Conditions (https://onlinelibrary.wiley.com/terms-and-conditions) on Wiley Online Library for rules of use; OA articles are governed by the applicable Cereative Commons. Licensecuted to the terms and Conditions (https://onlinelibrary.wiley.com/terms-and-conditions) on Wiley Online Library for rules of use; OA articles are governed by the applicable Cereative Commons. Licensecuted to the terms and conditions are governed by the applicable Cereative Commons.

Fig. 20. Vertical sections through vermicular structures in a cavity within a thrombolitic stromatolite. (A) to (C) Field views of a microbial bioherm; red box in (B) shows location of sample, from upper part of bioherm. (C) Field detail of microbial columns overlain by bedded limestone. (D) Whole thin section view of microbialite, showing abundant cavities. (E) Enlargement of red box in (D), showing cavities (darker grey with geopetals) in microbialite mass. (F) Detail of right side of (E), showing vermicular structure in geopetal fill. (G) to (I) Details of left side of (E) (yellow box) showing branched structure of light areas of sparite within micrite fill of cavity, interpreted as possible microburrow networks of meiofauna during shallow burial, and not as sponges. Uppermost Gushan Formation, upper Cambrian, Xiaweidian, near Beijing, China.

molecular-clock divergence-time estimates. Finally, there is a possibility that a selforganized fabric arose from the microbial production and subsequent decay of exopolymers (Défarge et al., 1996) superficially resembling spongin networks of some modern aspiculate sponges; however, such features are considered in this study as unlikely to be compatible with vermiform networks because exopolymer networks are two orders of magnitude smaller than vermiform fabrics. As an alternative, immiscible microfluids and respective capillary action might have evolved, that is syneresis in its broadest sense. The work of Turner (2021) is fascinating and provoking at the same time because there is a timing issue that concerns both the evolution of the interpreted sponges and the formation of the microfabric itself subsequent to the precipitation of marine cement from marine pore-waters. This is also an excellent example of a case where mesoscopic 3D reconstruction is eminently needed to provide basic information about a rather feature-poor microfabric.

# Potential pitfalls

Literature on keratose sponges in ancient carbonates reveals two common features: (i) all studies refer back to the original microscopic 2D and 3D reconstruction study by Luo & Reitner (2014); and (ii) in almost all cases, subsequent authors regarded these structures as actual sponges without adding their own evidence in support of the original interpretation. In addition, there are cases of unintended errors in reporting earlier studies, giving the impression of occurrence of sponges in other sequences, that were not stated in the cited works. A good example is in literature on Permian-Triassic boundary microbialite (PTBM) sequences. Ezaki et al. (2008, fig. 8C) illustrated a fabric described as "Highly amalgamated and interconnected areas exhibiting spongelike texture with infilling of peloids", cited by Friesenbichler et al. (2018,

p. 654) as an example of sponges in the PTBMs, yet Ezaki et al. (2008) did not say that these structures are sponges. Furthermore, the material illustrated by Ezaki et al. (2008, fig. 8) shows that all four images in that figure are actually partially altered portions of the lobate constructor of post-extinction microbialite microbialites in South China, now named as Calcilobes wangshenghaii (partly illustrated in Fig. 12G; also see Kershaw et al., 2021b), which is not a sponge; the interpreted sponge fabrics (e.g. Wu et al., 2021) refer to the sediment between the microbial frame-constructors, not the microbial frame itself. Figure 12E shows further complexity in the microbialite infills that do not resemble sponge fabrics. In PTBMs, Friesenbichler et al. (2018) and Heindel et al. (2018) recorded possible keratose sponges from Armenia, and Turkey and Iran, respectively; in both cases these are called keratose sponges by Lee & Riding (2021a, table 1). Many of the possible keratose sponges illustrated by Heindel et al. (2018), noted earlier, are simply carbonate mudstones-wackestones. Thus: (i) the notion of a 'sponge takeover' after the end-Permian extinction (Baud et al., 2021); and (ii) the Cambrian to Triassic correlation between possible keratose sponges and microbial reef carbonates (Lee & Riding, 2021a, fig. 9), that includes PTBMs, are considered here to be premature.

# Criteria for recognition of keratose sponges

Six criteria presented by Luo et al. (2022) are a valuable approach, summarized in Table 1 with detailed comments. However, even taken collectively, those criteria leave considerable uncertainty, even ambiguity, for verification of keratose sponges. The following three criteria present another approach: (i) A recognizable sponge body, which may include radial or other symmetries, water canals and/or a spongocoellike internal cavity. (ii) A plausible organic geometric relationship between the fibrous network

and outer boundary of the body, for example subparallel canals/network strands reaching the body surface (Fig. 1B). Even the most amorphous archaeocyaths (for example, *Retilamina*, Savarese & Signor, 1989) show such geometrical relationships, consistent with a sponge interpretation. Such features as (i) and (ii) may be recognizable using a series of closely-spaced parallel thin sections of a block containing suspected keratose sponge fabrics. (iii) Considering taphonomic and diagenetic processes discussed earlier in this study, geopetal fabrics within and between strands in a network would not be expected.

# Implications: The four settings

In the *Introduction* section, four settings of interpreted keratose sponges were presented, and broader aspects of each are stated below to provide perspective of the implications of this study.

- 1 Neoproterozoic keratose sponges were proposed by Turner (2021), therefore indicating the possible presence of such derived metazoans at 890 Ma, significantly earlier than the appearance of its parent taxon, the spongin-bearing demosponges which evolved in the late Cryogenian according to molecular clock divergence time estimates (Fig. 2), thus younger than the age of the material studied by Turner (2021). This age difference between the molecular clock model and the dated rocks warrants verification of a sponge affinity of the structures described by Turner (2021).
- 2 A consortium between proposed keratose sponges and benthic microbial communities, with introduction of the genetic term keratolite for the proposed sponge component was presented by Lee & Riding (2021a). A consortium (= community) asks for some kind of synecology whether symbiotic, mutual, commensal or even parasitic in nature. For sponges, this issue is extremely complex (Wilkinson, 1978; Cleary et al., 2019). For fossil material, without the application of supplementary multiproxy geochemical data at high resolution (N, S, O, C isotopes; biomarkers), such an approach must be considered problematic. The distinct sets of (interpreted) keratose sponges claimed to alternate with sets of microbialites in considerable lateral continuity (Lee & Riding, 2021a) implies mutual exclusiveness (time-controlled faciesorcontrolled) than a kind of consortium. Given the uncertainty regarding presence of sponges in a

variety of carbonate fabrics (this study), it is recommended that use of the term keratolite is suspended pending confirmation of the nature of respective fabrics.

- 3 Cambro-Ordovician occurrences of potential keratose sponges reported in numerous studies have importance for Palaeozoic evolution of the biosphere with impact on understanding the Great Ordovician Biodiversity Event, noted by Servais et al. (2021) to consist of an episode of change rather than a short-term event. If sponges occurred in larger abundance than has been recorded by verified sponges, then there is an important potential impact on the nature of ancient benthic assemblages across this period. Thus, it is critical to correctly identify the affinity of these structures before applying them in a wider context of palaeo-biodiversity.
- 4 Rapid and immense shifts in ecosystems after the end-Permian extinction include a short period of development of microbialites in shallow marine carbonate settings, the appearance and disappearance of which remain unexplained. However, recent contributions to literature of interpreted presence of keratose sponges has a significant impact on models of biotic and environmental change. The Permian-Triassic boundary microbialites are likely unique in the rock record (Kershaw et al., 2021b), so the notion of a concurrent sponge increase is critically influential in ecosystem analysis. Interpretation of keratose sponge expansion after the end-Permian mass extinction is an attractive idea, corresponding with possible sponge development during low-oxygen conditions associated with that extinction. Nevertheless, lack of verification of sponges in post-extinction facies means that it is not wise to include sponges in models. The corollary is that the unverified reports of sponge presence also lead to uncertainty in the nature of biotic assemblages. In a modern context, there is increase in sponges in modern coral reef systems that may be a reflection in the decline of corals, while sponges are more resilient to change (but see Perkins et al., 2022, for bleaching sponges). Sponge expansion after mass extinction is thus an area of great potential interest in understanding modern changes.

#### CONCLUSIONS

1 The interpretation of keratose sponges in carbonate facies through the Neoproterozoic to

3653919, 2023, 3, Downloaded from https://onlinelibrary.wiley.com/doi/10.1111/sed.13059 by Mount Holyoke College Library, Wiley Online Library on [02/01/2024]. See the Terms and Conditions (https://onlinelibrary.wiley.com/emers-and-conditions) on Wiley Online Library or rules of use; OA articles are governed by the applicable Creative Commons License

Jurassic (and maybe as late as Eocene) record produced numerous inconsistencies that concern timing, depositional and environmental context, biostratinomy and diagenesis. The interpretation is considered to be at best unsafe, and at worst incorrect.

- 2 The issue requires three-dimensional reconstructions at mesoscopic scale of the microfabrics in scope to illustrate and distinguish a distinct body fossil from post-depositional features related to, for example, fluid capture, burrows, meiofaunal activity or local diagenesis. Two-dimensional thin section studies alone are insufficient to verify the presence of keratose sponges.
- 3 If mesoscopic reconstruction results in a discrete body fossil, for the interpretation of a keratose sponge, automicrite needs to be identified, and likely the preservation of a sponge-specific canal system associated with distinct cortical boundaries.

#### **ACKNOWLEDGEMENTS**

During development of this study we are very grateful for discussions with Andrej Pisera (Warsaw), who made valuable comments on an earlier version of the manuscript, and provided the image used in Fig. 3H. Rachel Wood is thanked for comments and advice in an earlier version. Lisa Amati (New York State Museum) kindly sent the original Cryptozoön material to FN. Marc Choquette (Université Laval) is thanked for XRD analysis of a Cryptozoön sample illustrated in Fig. 10. Comments from two anonymous reviewers, Joe Botting (as journal reviewer), Marcelo Carrera, Cristina Diaz, Dirk Erpenbeck, Jonsung Hong, Noel James, Dirk Knaust, Jino Park, Christine Schönberg, Elizabeth Turner, Max Wisshak and Gert Wörheide have provided much insight into this study. FN thanks Félix Gagnon and Edmond Rousseau (Laval University) for technical assistance. SK thanks: Haizhou Wang (China University of Petroleum) for access to Cambrian carbonates in North China; Yue Li (Nanjing Institute) for access to Silurian carbonates in South China; and Robert Riding (Tennessee) for access to Cambro-Ordovician carbonates in Utah. CS also thanks: Lucie Goodayle, Natural History Museum, London, Science Photographer for Vauxia images; Tom White and Javier Ignacio Sánchez Almazán, from Natural History Museum, London, and National Museum of Natural Sciences, Madrid,

respectively, for access to Recent sponges. AM thanks Yuandong Zhang (Nanjing Institute) for access to the Ordovician carbonates in NW China. We gratefully acknowledge information on microburrows provided by Klaudiusz Salamon, who sadly died in early 2022.

#### CONFLICT OF INTEREST

There are no conflicts of interest.

#### DATA AVAILABILITY STATEMENT

Not applicable.

#### REFERENCES

- Antcliffe, J.B., Callow, R.H.T. and Brasier, M.D. (2014) Giving the early fossil record of sponges a squeeze. *Biol. Rev.*, **89**, 972–1004.
- Aragonés Suarez, P. and Leys, S. (2022) The sponge pump as a morphological character in the fossil record. *Paleobiology*, 1–16.
- Awramik, S.M. and Grey, K. (2005) Stromatolites: biogenicity, biosignatures, and bioconfusion. In: Astrobiology and Planetary Missions (Eds Hoover, R.B., Levin, G.V., Rozanov, A.Y. and Gladstone, G.R.), Proceedings of SPIE, The international society for optics and photonics, 5906, 9.
- Ax, P. (1996) Multicellular Animals: A New Approach to the Phylogenetic Order in Nature. Springer, New York, 1, 225 pp.
- Baliński, A., Sun, Y. and Dzik, J. (2013) Traces of marine nematodes from 470 million years old early Ordovician rocks in China. Nematology, 15, 567–574.
- Bathurst, R.G.C. (1975) Carbonate Sediments and their Diagenesis. Elsevier, Amsterdam, 658 pp.
- Bathurst, R.G.C. (1982) Genesis of stromatactis cavities between submarine crusts in Palaeozoic carbonate mud buildups. *J. Geol. Soc. London*, **139**, 165–181.
- Baud, A., Richoz, S., Brandner, R., Krystyn, L., Heindel, K., Mohtat, T., Mohtat-Aghai, P. and Horacek, M. (2021) Sponge takeover from end-Permian mass extinction to early Induan time: Records in Central Iran Microbial Buildups. Front. Earth Sci., 9, 586210.
- Biddle, S.K., LaGrange, M.T., Harris, B.S., Fiess, K., Terlaky, V. and Gingras, M.L. (2021) A fine detail physico-chemical depositional model for Devonian organic-rich mudstones: a petrographic study of the hare Indian and Canol formations, Central Mackenzie Valley, Northwest Territories. Sediment. Geol., 414, 27.
- Bobrovskiy, I., Hope, J.M., Nettersheim, B.J., Volkman, J.K., Hallmann, C. and Brocks, J.J. (2020) Algal origin of sponge sterane biomarkers negates the oldest evidence for animals in the rock record. *Nat. Ecol. Evol.*, **5**, 165–168.
- Bonaglia, S., Nascimento, F.J.A., Bartoli, M., Klawonn, I. and Brüchert, V. (2014) Meiofauna increases bacterial denitrification in marine sediments. *Nat. Commun.*, **5**, 5133.

- Botting, J.P. (2005) Exceptionally well-preserved middle Ordovician from the Llandegley rocks lagerstätte, Wales. *Palaeontology*, **48**, 577–617.
- Botting, J.P., Janussen, D., Muir, L.A., Dohrmann, M., Ma, J. and Zhang, Y. (2022) Extraordinarily early Venus' flower basket sponges (Hexactinellida, Euplectellidae) from the uppermost Ordovician Anji biota, China. *Palaeontology*, 65, e12592.
- Botting, J.P. and Muir, L.A. (2018) Early sponge evolution: a review and phylogenetic framework. *Palaeoworld*, 27, 1–29.
- Botting, J.P., Muir, L.A. and Lin, J.-P. (2013) Relationships of the cambrian protomonaxonida (Porifera). *Palaeontol. Electron.*, **16**, 23.
- Botting, J.P., Muir, L.A., Zhang, Y., Ma, X., Ma, J., Wang, L., Zhang, K., Song, Y. and Fang, X. (2017) Flourishing sponge-based ecosystems after the end-Ordovician mass extinction. Curr. Biol., 27, 556–562.
- Bourillot, R., Vennin, E., Dupraz, C., Pace, A., Foubert, A., Rouchy, J.-M., Patrier, P., Blanc, P., Bernard, D., Lesseur, J. and Visscher, P.T. (2020) The record of environmental and microbial signatures in ancient Microbialites: the terminal carbonate complex from the Neogene basins of southeastern Spain. Minerals, 10, 276.
- Bourque, P.-A. and Boulvain, F. (1993) A model for the origin and Petrogenesis of the red Stromatactis limestone of Paleozoic carbonate mounds. *J. Sediment. Res.*, **63**, 607–619.
- Bourque, P.-A. and Gignac, H. (1983) Sponge-constructed stromatactis mud mounds, Silurian of Gaspé, Québec. *J. Sediment. Petrol.*, **53**, 521–532.
- Bowerbank, J.S. (1862) On the anatomy and physiology of the Spongiadae. Part III. On the generic characters, the specific characters, and on the method of examination. *Philos. Transac. R. Soc. London*, **152**, 1087–1135.
- Brachert, T.C., Dullo, W.C. and Stoffers, P. (1987)
  Diagenesis of siliceous sponge limestones from the Pleistocene of the Tyrrhenian Sea (Mediterranean Sea). Facies, 17, 41–49.
- Brayard, A., Vennin, E., Olivier, N., Bylund, K.G., Jenks, J., Stephen, D.A., Bucher, H., Hofmann, R., Goudemand, N. and Escarguel, G. (2011) Transient metazoan reefs in the aftermath of the end-Permian mass extinction. Nat. Geosci., 4, 693–697.
- Bromley, R.G. and Schönberg, C.H. (2008) Borings, bodies and ghosts: spicules of the endolithic sponge *aka akis* sp. nov. within the boring *Entobia cretacea*, cretaceous, England. In: *Current Developments in Bioerosion* (Eds Wisshak, M. and Tapanila, L.), Erlangen Earth Conference Series. Springer, Berlin, Heidelberg.
- Butterfield, N.J. and Nicholas, C.J. (1996) Burgess shale-type preservation of both non-mineralizing and 'shelly' Cambrian organisms from the Mackenzie Mountains, northwestern Canada. *J. Paleo.*, **70**, 893–899.
- Carrera, M.G. and Botting, J.P. (2008) Evolutionary history of Cambrian spiculate sponges: implication for the Cambrian evolutionary fauna. *Palaios*, 23, 124–138.
- Carter, H.J. (1875) Notes introductory to the study and classification of the Spongida. Part II. Proposed classification of the Spongida. Ann. Mag. Nat. Hist., 4(16), 126–145.
- Cleary, D.F.R., Ferreira, M.R.S., Bat, N.K., Moura Polónia, A.R., Marcial Gomes, N.C. and de Voogd, N.J. (2019) Bacterial composition of sponges, sediment and seawater in enclosed and open marine lakes in Ha Long Bay Vietnam. *Mar. Biol. Res.*, 16, 18–31.

- Cloud, P. (1973) Pseudofossils: a plea for caution. Geology, 1, 123–127.
- Conway Morris, S. and Whittington, H.B. (1985) Fossils of the burgess shale. *Geol. Survey Canada*, **43**, 1–31.
- Cullen, D. (1973) Bioturbation of superficial marine sediments by interstitial meiobenthos. *Nature*, 242, 323–324.
- De Freitas, T.A. (1991) Ludlow (Silurian) lithistid and hexactinellid sponges, Cape Phillips formation, Canadian Arctic. Can. J. Earth Sci., 28, 2042–2061.
- De Voogd, N.J., Alvarez, B., Boury-Esnault, N., Carballo, J.L., Cárdenas, P., Díaz, M.-C., Dohrmann, M., Downey, R., Hajdu, E., Hooper, J.N.A., Kelly, M., Klautau, M., Manconi, R., Morrow, C.C., Pisera, A.B., Ríos, P., Rützler, K., Schönberg, C., Vacelet, J. and van Soest, R.W.M. (2022) World Porifera Database. https://www.marinespecies.org/.
- Debrenne, F. (1999) The past of sponges, sponges of the past. Mem. Queensl. Mus., 44, 9–21.
- Debrenne, F., Gandin, A. and Rowland, S.M. (1989) Lower Cambrian bioconstructions in northwestern Mexico (Sonora). Depositional setting, paleoecology and systematics of Archaeocyaths. *Geobios*, **22**, 137–195.
- Défarge, C., Trichet, J., Jaunet, A.-M., Robert, M., Tribble, J. and Sansone, F.J. (1996) Texture of microbial sediment revealed by cryo-scanning electron microscopy. *J. Sediment. Res.*, **66**, 935–947.
- Dickson, J.A.D. (1978) Neomorphism and recrystallization.
  In: Encyclopedia of Sediments and Sedimentary Rocks
  (Eds Middleton, G.V., Church, M.J., Coniglio, M., Hardie,
  L.A. and Longstaffe, F.J.), Encyclopedia of Earth Sciences
  Series. Springer, Dordrecht.
- Dohrmann, M. and Wörheide, G. (2017) Dating early animal evolution using phylogenomic data. *Sci. Rep.*, 7, 3599.
- Ehrlich, H. (2019) Marine Biological Materials of Invertebrate Origin. Springer, Berlin, Heidelberg, 329 pp.
- Ehrlich, H., Rigby, J.K., Botting, J.P., Tsurkan, M.V., Werner, C., Schwille, P., Petrasek, Z., Pisera, A., Simon, P., Sivkov, V.N., Vyalikh, D.V., Molodtsov, S.L., Kurek, D., Kammer, M., Hunoldt, S., Born, R., Stawski, D., Steinhof, A., Bazhenov, V.V. and Geisler, T. (2013) Discovery of 505-million-year old chitin in the basal demosponge Vauxia gracilenta. Sci. Rep., 3, 3497.
- Ehrlich, H., Wysokowski, M., Zółtowska-Aksamitowska, S., Petrenko, I. and Jesionowski, T. (2018) Collagens of Poriferan origin. *Mar. Drugs.* 16, 79.
- Erpenbeck, D., Sutcliffe, P., Cook, S., Dietzel, A., Maldonado, M., van Soest, R.W.M., Hooper, J.N.A. and Wörheide, G. (2012) Horny sponges and their affairs: on the phylogenetic relationships of keratose sponges. *Mol. Phylogenet. Evol.*, **63**, 809–816.
- Erpenbeck, D. and van Soest, R.W.M. (2007) Status and perspective of sponge chemosystematics. *Marine Biotechnol.*, **9**, 2–19.
- Exposito, J.-Y., Le Guellec, D., Lu, Q. and Garrone, R. (1991) Short chain collagens in sponges are encoded by a family of closely related genes. *J. Biol. Chem.*, **286**, 21923–21928.
- Ezaki, Y., Liu, J., Nagano, T. and Adachi, N. (2008) Geobiological aspects of the earliest Triassic microbialites along the southern periphery of the tropical Yangtze platform: initiation and cessation of a microbial regime. *Palaios*, 23, 356–369.
- Fan, W., Zhao, Y., Chen, A., You, X. and Cong, P. (2021) New vauxiid sponges from the Chengjiang biota and their evolutionary significance. *J. Geol. Soc. London*, **178**, jgs2020-162.

- Flügel, E. (2004) Microfacies in Carbonate Rocks; Analysis, Interpretation and Application. Springer, Berlin, Heidelberg; New York, NY, 976 pp.
- Folk, R.L. (1965) Some aspects of recrystallisation in ancient limestones. In: Dolomitization and Limestone Diagenesis (Eds Pray, L.C. and Murray, R.C.), Special Publication of Society of Economic Paleontologists and Mineralogists, 13, 14–48.
- Friedman, G.M. (2000) Late Cambrian cabbage-head stromatolites from Saratoga Springs, New York, USA. Carbonates Evaporites, 15, 37–48.
- Friesenbichler, E., Richoz, S., Baud, A., Krystyn, L., Sahakyan, L., Vardanyan, S., Peckmann, J., Reitner, J. and Heindel, K. (2018) Sponge-microbial buildups from the lowermost Triassic Chanakhchi section in southern Armenia: microfacies and stable carbon isotopes. *Palaeogeogr. Palaeoclimatol. Palaeoecol.*, 490, 653–672.
- Fritz, G.K. (1958) Schwammstotzen, Tuberolithe und Schuttbreccien im Weißen Jura der Schwäbischen Alb. Arbeiten aus dem Geologisch-Palaontologischen Institut der Technischen Hochschule, Stuttgart, Neue Folge, 13, 1– 119
- Froget, C. (1976) Observations sur l'altération de la silice et des silicates au cours de la lithification carbonatée (Région Siculo-Tunisienne). Géologie Méditerranéenne, 3, 219–225.
- Garrone, R. (1978) Phylogenesis of Connective Tissue: Morphological Aspects and Biosynthesis of Sponge Intercellular Matrix. JohnWiley & Sons, Hoboken, NJ, USA.
- Gazave, E., Lapébie, P., Ereskovsky, A., Vacelet, J., Renard, E., Cardenas, P. and Borchiellini, C. (2012) No longer Demospongiae: Homoscleromorph formal nomination as a fourth class of Porifera. *Hydrobiologia*, 687, 3–10.
- Giere, O. (2009) Meiobenthology; the Microscopic Motile Fauna of Aquatic Sediments, 2nd edn. Springer, Berlin.
- Gischler, E., Fuchs, A., Bach, W. and Reitner, J. (2021) Massive cryptic microbe-sponge deposits in a Devonian fore-reef slope (Elbingerode reef complex, Harz Mts., Germany). *Paläontologische Zeitschrift*, **95**, 683–707.
- Goldring, W. (1938) Algal barrier reefs in the lower Ozarkian of New York with a chapter on the importance of coralline algae as reef builders through the ages. *Bull. N.Y. State* Mus., 315, 5–75.
- Goldring, R., Pollard, J.E. and Taylor, A.M. (1991) Anconichnus horizontalis: a pervasive ichnofabric-forming trace fossil in post-Paleozoic offshore siliciclastic facies. Palaios, 6, 250–263.
- Göthel, H. (1992) Guide de la faune sous-marine: La Méditerranée. Invertébrés marins et poissons. Eygen Ulmer GmbH & Co, Stuttgart, 318 pp.
- Gray, J.E. (1867) Notes on the arrangement of sponges, with the descriptions of some new genera. Proc. Zoolog. Soc. London, 2, 492–558.
- Grotzinger, J. and Rothman, D. (1996) An abiotic model for stromatolite morphogenesis. *Nature*, 383, 423–425.
- Guilini, K., Soltwedel, T., van Oevelen, D. and Vanreusel, A. (2011) Deep-sea nematodes actively colonise sediments, irrespective of the presence of a pulse of organic matter: result from an *in-situe* experiment. PLOS One, 6, e18912.
- Gupta, N.S. and Briggs, D.E.G. (2011) Taphonomy of animal organic skeletons through time. In: *Taphonomy. Aims & Scope*, Vol. 32 (Eds Allison, P.A. and Bottjer, D.J.). Springer, Dordrecht.
- Gürich, G. (1906) Les spongiostromides du Viséen de la Province de Namur. Mem. R. Belgian Mus. Nat. Sci., 3, 1–55.

- Gutzmer, J., Schaefer, M.O. and Beukes, N.J. (2002) Red bed-hosted oncolitic manganese ore of the Paleoproterozoic Soutpansberg group, Bronkhorstfontein, South Africa. Econ. Geol., 97, 1151–1166.
- Heindel, K., Foster, W.J., Richoz, S., Birgel, V.J., Roden, D.,
  Baud, A., Brandner, R., Krystyn, L., Mohtat, T., Kosun, E.,
  Twitchett, R., Reitner, J. and Peckmann, J. (2018) The formation of microbial-metazoan bioherms and biostromes following the latest Permian mass extinction. Gondw. Res.,
  61, 187–202.
- Hofmann, H.J. (1972) Precambrian remains in Canada: fossils, dubiofossils, and pseudofossils. *International Geological Congress*, 24th Session, Montreal, Proceedings of Section 1, 20–30.
- James, N.P. and Jones, B. (2015) Origin of Carbonate Sedimentary Rocks. American Geophysical Union, Wiley Works, Hoboken, 464 pp.
- Jenner, R.A. and Littlewood, D.T.J. (2008) Problematica old and new. Philos. Transac. R. Soc. London B: Biol. Sci., 363, 1503–1512.
- Jesionowski, T., Norman, M., Żółtowska-Aksamitowska, S., Petrenko, I., Joseph, Y. and Ehrlich, H. (2018) Marine Spongin: naturally prefabricated 3D scaffold-based biomaterial. Mar. Drugs, 16, 88.
- Junqua, S., Robert, L., Garrone, R., Pavans De Ceccatty, M. and Vacelet, J. (1974) Biochemical and morphological studies on the collagens of horny sponges. *Ircinia* filaments compared to spongines. *Connect. Tissue Res.*, 2, 193–203.
- Kamenskaya, O.E., Gooday, A.J., Tendal, O.S. and Melnik, V.F. (2015) Xenophyophores (Protista, foraminifera) from the clarion-Clipperton fracture zone with description of three new species. *Mar. Biodivers.*, 45, 581–593.
- Kenny, N.J., Francis, W.R., Rivera-Vicéns, R.E., Juravel, K., de Mendoza, A., Díez-Vives, C., Lister, R., Bezares-Calderón, L.A., Grombacher, L., Roller, M., Barlow, L., Camilli, S., Ryan, J., Wörheide, G., Hill, A., Riesgo, A. and Leys, S. (2020) Tracing animal genomic evolution with the chromosomal-level assembly of the freshwater sponge *Ephydatia muelleri*. *Nat. Commun.*, 11, 3676.
- Kershaw, S. (2000) Quaternary reefs of northeastern Sicily: structure and growth controls in an unstable tectonic setting. J. Coast. Res., 16, 1037–1062.
- Kershaw, S., Guo, L. and Braga, J.-C. (2005) A Holocene coral-algal reef at Mavra Litharia, gulf of Corinth, Greece: structure, history and applications in relative sea-level change. Mar. Geol., 215, 171–192.
- Kershaw, S., Li, Q. and Li, Y. (2021a) Addressing a Phanerozoic carbonate facies conundrum—sponges or clotted micrite? Evidence from early Silurian reefs, South China block. *Sediment. Rec.*, 19, 3–10.
- Kershaw, S., Zhang, T. and Li, Y. (2021b) Calcilobes wangshenghaii n. gen., n. sp., microbial constructor of Permian-Triassic boundary microbialites of South China, and its place in microbialite classification. Facies, 67, 28.
- Knaust, D. (2007) Meiobenthic trace fossils as keys to the Taphonomic history of shallow-marine Epicontinental carbonates. In: Trace Fossils Concepts, Problems, Prospects (Ed. Miller, W., III), pp. 502–517. Geology Department Humboldt State University Arcata, Arcata, CA.
- Knaust, D. (2010) Meiobenthic trace fossils comprising a miniature ichnofabric from late Permian carbonates of the Oman Mountains. Palaeogeogr. Palaeoclimatol. Palaeoecol., 286, 81–87.

- Knaust, D. (2021) Foraging flatworms and roundworms caught in the act: examples from a middle Triassic mud flat in Germany. Lethaia, 54, 495–503.
- Knoll, A.H. (2003) Biomineralization and evolutionary history. Rev. Mineral. Geochem., 54, 329–356.
- Kris, A. and McMenamin, M.A.S. (2021) Putative Proterozoic sponge spicules reinterpreted as microburrows. Academia Lett., 3800.
- Lakshtanov, L.Z. and Stipp, S.L.S. (2010) Interaction between dissolved silica and calcium carbonate: 1. Spontaneous precipitation of calcium carbonate in the presence of dissolved silica. Geochimica et Cosmochimica Acta, 74, 2655–2664.
- Lee, J.-H., Chen, J., Choh, S.-J., Lee, D.-J., Han, Z. and Chough, S.K. (2014) Furongian (late Cambrian) spongemicrobial maze-like reefs in the North China platform. *Palaios*, 29, 27–37.
- Lee, J.-H., Cho, S.-H., Jung, D.-Y., Choh, S.-J. and Lee, D.-J. (2021) Ribbon rocks revisited: the upper Cambrian (Furongian) Hwajeol formation, Taebaek group, Korea. Facies, 67, 19.
- Lee, J.-H. and Hong, J. (2019) Sedimentologic and paleoecologic implications for keratose-like sponges in geologic records. *J. Geol. Soc. Korea*, **55**, 735–748.
- Lee, J.-H. and Riding, R. (2021a) Keratolite-stromatolite consortia mimic domical and branched columnar stromatolites. *Palaeogeogr. Palaeoclimatol. Palaeoecol.*, 571 10288
- Lee, J.-H. and Riding, R. (2021b) The 'classic stromatolite' Cryptozöon is a keratose sponge-microbial consortium. Geobiology, 19, 189–198.
- Lee, J.-H. and Riding, R. (2022) Recognizing sponge in Spongiostroma Gürich, 1906 from the Mississippian of Belgium. J. Paleo., 12.
- Lee, J.-H. and Riding, R. (2023) Stromatolite-rimmed thrombolite columns and domes constructed by microstromatolites, calcimicrobes and sponges in late Cambrian biostromes, Texas, USA. Sedimentology, 70, 293–334.
- Lees, A. and Miller, J. (1995) Waulsortian banks. In: Carbonate Mud-Mounds, their Origin and Evolution (Eds Monty, C.L.V., Bosence, D.W.J., Bridges, P.H. and Pratt, B.R.), Special Publications of the International Association of Sedimentologists, 23, 191–271.
- Löhr, S.C. and Kennedy, M.J. (2015) Micro-trace fossils reveal pervasive reworking of Pliocene sapropels by low-oxygen-adapted benthic meiofauna. *Nat. Commun.*, 6, 1–8
- Lokier, S.W. and Al Junaibi, M. (2016) The petrographic description of carbonate facies: are we all speaking the same language? Sedimentology, 63, 1843–1885.
- Love, G.D., Grosjean, E., Stalvies, C., Fike, D.A., Grotzinger, J.P., Bradley, A.S., Kelly, A.E., Bhatia, M., Meredith, W., Snape, C.E., Bowring, S.A., Condon, D.J. and Summons, R.E. (2009) Fossil steroids record the appearance of Demospongiae during the Cryogenian period. *Nature*, 457, 718–721.
- Luo, C. (2015) "Keratose" Sponge Fossils and Microbialites: A Geobiological Contribution to the Understanding of Metazoan Origin. Unpublished PhD thesis. University of Göttingen, Göttingen, 151 pp.
- Luo, C., Pei, Y., Richoz, S., Li, Q. and Reitner, J. (2022) Identification and current palaeobiological understanding of "Keratosa"-type nonspicular demosponge fossils in

- carbonates: with a new example from the lowermost Triassic, Armenia. *Life*, **12**, 1348.
- Luo, C. and Reitner, J. (2014) First report of fossil "keratose" demosponges in Phanerozoic carbonates: preservation and 3-D reconstruction. *Naturwissenschaften*, 101, 467–477.
- Luo, C. and Reitner, J. (2016) 'Stromatolites' built by sponges and microbes-a new type of Phanerozoic bioconstruction. Lethaia, 49, 555-570.
- **Macintyre, I.G.** (1978) Distribution of submarine cements in a modern Caribbean fringing reef, Galeta point, Panama; reply. *J. Sediment. Res.*, **48**, 669–670.
- Macintyre, I.G. (1985) Submarine cements—the peloidal question. SEPM Spec. Public., 36, 109–116.
- Maldonado, M. (2009) Embryonic development of verongid demosponges supports the independent acquisition of spongin skeletons as an alternative to the siliceous skeleton of sponges. *Biol. J. Linn. Soc.*, **97**, 427–447.
- Manconi, R., Cadeddu, B., Ledda, F. and Pronzato, R. (2013)

  An overview of the Mediterranean cave-dwelling horny sponges (Porifera, Demospongiae). *ZooKevs.* 281, 1–68.
- Manconi, R., Cubeddu, T., Pronzato, R., Sanna, M.A., Nieddu, G., Gaino, E. and Stocchino, G.A. (2022) Collagenic architecture and morphotraits in a marine basal metazoan as a model for bioinspired applied research. J. Morphol., 2022, 1–20.
- Matysik, M. (2016) Facies types and depositional environments of a morphologically diverse carbonate platform: a case study from the Muschelkalk (middle Triassic) of upper Silesia, southern Poland. *Ann. Soc. Geol. Pol.*, **86**, 119–164.
- Matysik, M., Stemmerik, L., Olaussen, S. and Brunstad, H. (2018) Diagenesis of spiculites and carbonated in a Permian temperate ramp succession Tempelfjorden Group, Spitsbergen, Arctic Norway. Sedimentology, 65, 745–774.
- Matysik, M., Stemmerik, L., Olaussen, S., Rameil, N., Gianotten, I.P. and Brunstad, H. (2021) Cherts, spiculites, and collapse breccias porosity generation in upper Permian reservoir rocks, Gohta discovery, Loppa high, South-Western Barents Sea. *Mar. Petrol. Geol.*, **128**, 105043.
- McIlroy, D. (2022) Were the first trace fossils really burrows or could they have been made by sediment-displacive chemosymbiotic fossils? *Life*, 12, 136.
- McMahon, S. and Cosmidis, J. (2021) False biosignatures on Mars: anticipating ambiguity. *J. Geol. Soc. London*, **179**, 1–25.
- McMahon, S., Hood, A. and McIlroy, D. (2017) Origin and occurrence of subaqueous sedimentary cracks. In: Earth System Evolution and Early Life: A Celebration of the Work of Martin Brasier (Eds Brasier, A.T., McIlroy, D. and McLoughlin, N.), Geol. Soc. Lond. Spec. Publ, 448, 285–309.
- McMahon, S., Ivarsson, M., Wacey, D., Saunders, M., Belivanova, V., Muirhead, D., Knoll, P., Steinbock, O. and Frost, D.A. (2021) Dubiofossils from a Mars-analogue subsurface palaeoenvironment: the limits of biogenicity criteria. *Geobiology*, **19**, 473–488.
- McMenamin, M.A.S. (2016) Parenting skills. In: *Dynamic Paleontology: Using Quantification and Other Tools to Decipher the History of Life* (Ed. McMenamin, M.A.S.), pp. 191–205. Springer, Cham.
- Monty, C. (1981) Phanerozoic Stromatolites: Case Histories. Springer-Verlag, Berlin, Heidelberg, New York, NY, 249 pp.

- Moore, C.H. (2001) Carbonate Reservoirs: Porosity Evolution and Diagenesis in a Sequence Stratigraphic Framework. Elsevier Science, Amsterdam, 460 pp.
- Morrow, C. and Cárdenas, P. (2015) Proposal for a revised classification of the Demospongiae (Porifera). Front. Zool., 12. 7–27.
- Munnecke, A., Westphal, H., Reijmer, J.J.G. and Samtleben, C. (1997) Microspar development during early marine burial diagenesis: a comparison of Pliocene carbonates of The Bahamas with Silurian limestones from Gotland (Sweden). Sedimentology, 44, 977–990.
- Neira, C., Sellanes, J., Levin, L.A. and Arntz, W.E. (2001) Meiofaunal distributions on the Peru margin: relationship to oxygen and organic matter availability. *Deep-Sea Res.*, 48, 2453–2472.
- Nettersheim, B.J., Brocks, J.J., Schwelm, A., Hope, J.M., Not, F., Lomas, M., Schmidt, C., Schiebel, R., Nowack, E.C.M., DeDeckker, P., Pawlowski, J., Bowser, S.S., Bobrovskiy, I., Zonnefeld, K., Kucera, M., Stuhr, M. and Hallmann, C. (2019) Putative sponge biomarkers in unicellular Rhizaria question and early rise of animals. Nat. Ecol. Evol., 3, 577-581.
- Neuweiler, F., Bourque, P.-A. and Boulvain, F. (2001) Why is stromatactis so rare in Mesozoic carbonate mud mounds? *Terra Nova*, **13**, 338–346.
- Neuweiler, F. and Burdige, D.J. (2005) The modern calcifying sponge Spheciospongia vesparium, (Lamarck, 1815), great Bahama Bank: implications for ancient sponge mud-mounds. Sediment. Geol., 175, 89–98.
- Neuweiler, F., Daoust, I., Bourque, P.-A. and Burdige, J.B. (2007) Degradative calcification of a modern siliceous sponge from the great Bahama Bank, The Bahamas: a guide for interpretation of ancient sponge-bearing limestones. *J. Sediment. Res.*, 77, 552–563.
- Neuweiler, F., d'Orazio, V., Immenhauser, A., Geipel, G., Heise, K.-H., Cocozza, C. and Miano, T.M. (2003) Fulvic acid-like organic compounds control nucleation of marine calcite under suboxic conditions. *Geology*, 31, 681-684.
- Neuweiler, F., Gautret, P., Thiel, V., Lange, R., Michaelis, W. and Reitner, J. (1999) Petrology of lower cretaceous carbonate mud mounds (Albian, N. Spain): insights into organomineralic deposits of the geological record. Sedimentology, 46, 837–859.
- Neuweiler, F., Rutsch, M., Geipel, G., Reimer, A. and Heise, K.-H. (2000) Soluble humic substances from in situ precipitated microcrystalline calcium carbonate, internal sediment, and spar cement in a cretaceous carbonate mudmound. Geology, 28, 851–854.
- Neuweiler, F., Turner, E.C. and Burdige, D.J. (2009) Early Neoproterozoic origin of the metazoan clade recorded in carbonate rock texture. *Geology*, **37**, 475–478.
- Park, J., Lee, J.-H., Hong, J., Choh, D.-C. and Lee, D.-J. (2015) An upper Ordovician sponge-bearing micritic limestone and implication for early Palaeozoic carbonate successions. Sediment. Geol., 319, 124–133.
- Park, J., Lee, J.-H., Hong, J., Choh, S.-J., Lee, D.-C. and Lee, D.-J. (2017) Crouching shells, hidden sponges: unusual late Ordovician cavities containing sponges. Sediment. Geol., 347, 1–9.
- Parry, L.A., Boggiano, P.C., Condon, D.J., Garwood, R.J., de M. Leme, J., McIlroy, D., Brasier, M., Trindade, R., Campanha, G.A.C., Pacheco, M.L.A.F., Diniz, C.Q.C. and Liu, A. (2017) Ichnological evidence for meiofaunal

- bilaterians from the terminal Ediacaran and earliest Cambrian of Brazil. *Nat. Ecol. Evol.*, 1, 1455–1464.
- Pei, Y., Duda, J.-P., Schönig, J., Luo, C. and Reitner, J. (2021) Late Anisian microbe-metazoan build-ups in the Germanic Basin: aftermath of the Permian-Triassic crisis. *Lethaia*, 54, 823–844. https://doi.org/10.1111/let. 12442.
- Pei, Y., Hagdorn, H., Voigt, T., Duda, J.-P. and Reitner, J. (2021) Palaeoecological implications of lower-middle Triassic stromatolites and microbe-metazoan build-ups in the Germanic Basin: insights into the aftermath of the Permian-Triassic crisis. *Geosciences*, 12, 133.
- Pemberton, S.G. and Gingras, M.K. (2005) Classification and characterizations of biogenically enhanced permeability. Am. Assoc. Petrol. Geol. Bull., 89, 1495–1517.
- Pemberton, S.G., MacEachern, J.A., Gingras, M.K. and Saunders, T.D.A. (2008) Biogenic chaos: Cryptobioturbation and the work of sedimentologically friendly organisms. *Palaeogeogr. Palaeoclimatol. Palaeoecol.*, **270**, 273–279.
- Perkins, N.R., Monk, J., Soler, G., Gallagher, P. and Barrett, N.S. (2022) Bleaching in sponges on temperate mesophotic reefs observed following marine heatwave events. *Climate Change Ecol.*, 3, 100046.
- Pham, D., Hong, J. and Lee, J. (2021) Keratose sponge—microbial consortia in stromatolite-like columns and thrombolite-like mounds of the lower Ordovician (Tremadocian) Mungok formation, Yeongwol, Korea. *Palaeogeogr. Palaeoclimatol. Palaeoecol.*, **572**, 110409.
- Pike, J., Bernhard, J.M., Moreton, S.G. and Butler, I.B. (2001) Microbioirrigation of marine sediments in dysoxic environments: implications for early sediment fabric formation and diagenetic processes. *Geology*, 29, 923– 926.
- Pisera, A. (1997) Upper Jurassic siliceous sponges from the Swabian Alb: taxonomy and paleoecology. *Palaeontol. Polonica*, 57, 3–216.
- Pisera, A. (2004) What can we learn about siliceous sponges from palaeontology. Bolletino Museo Istituto Biologia Università Genova, 68, 55–69.
- Pourret, O., Davranche, M., Gruau, G. and Dia, A. (2007) Competition between humic acid and carbonates for rare earth elements complexation. *J. Colloid Interface Sci.*, **305**, 25–31.
- **Reitner**, J. (1993) Modern cryptic microbialite/metazoan facies from Lizard Island (great barrier reef, Australia) formation and concepts. *Facies*, **29**, 3–39.
- Reitner, J., Hühne, C. and Thiel, V. (2001) Porifera-rich mud mounds and microbialites as indicators of environmental changes within the Devonian/lower carboniferous critical interval. *Terra Nostra*, 4, 60–65.
- Reitner, J. and Keupp, H. (1991) The fossil record of the Haplosclerid excavating sponge aka de Laubenfels. In: Fossil and Recent Sponges (Eds Reitner, J. and Keupp, H.), pp. 102–120. Springer-Verlag, Berlin, Heidelberg.
- Reitner, J., Luo, C., Suarez-Gonzalez, P. and Duda, J.-P. (2021) Revisiting the phosphorite deposit of Fontanarejo (Central Spain): new window into the early Cambrian evolution of sponges and the microbial origin of phosphorites. Special Issue 7: THEMATIC ISSUE: The Ediacaran System and the Ediacaran-Cambrian Transition. *Geol. Mag.*, **159**, 1220–1239. https://doi.org/10.1017/S001675682100087X.

- Reitner, J. and Wörheide, G. (2002) Non-lithistid fossil Demospongiae: origins of their palaeobiodiversity and highlights in history of preservation. In: *Systema Porifera:* A Guide to the Classification of Sponges (Eds Hooper, J.N.A. and van Soest, R.W.M.), pp. 52–68. Kluwer Academic/Plenum Publishers, New York, NY.
- **Retallack, G.J.** (2015) Reassessment of the Silurian problematicum. *Rutgersella as another post-Ediacaran vendobiont, Alcheringa*, **39**, 573–588.
- Rigby, J.K., Rohr, D.M., Blodgett, R.B. and Britt, B.B. (2008) Silurian sponges and some associated fossils from the Heceta limestone, Prince of Wales Island, southeastern Alaska. *J. Paleo.*, 82, 91–101.
- Rützler, K. and Richardson, S. (1996) The Caribbean spicule tree: a sponge-imitating foraminifer (Astrorhizidae). Bulletin de l'Institut Royal des Sciences Naturales de Belgique, Biologie Supplement, 66, 143–151.
- Savarese, M. and Signor, P.W. (1989) New archaeocyathan occurrences in the upper Harkless formation (lower Cambrian of western Nevada). J. Paleo., 63, 539–549.
- Schaefer, M.O., Gutzmer, J. and Beukes, N.J. (2001) Late Paleoproterozoic Mn-rich oncoids: earliest evidence for microbially mediated Mn precipitation. *Geology*, **29**, 835– 838
- Schieber, J., Southard, J.B., Kissling, P., Rossman, B. and Ginsburg, R. (2013) Experimental deposition of carbonate mud from moving suspensions: importance of flocculation and implications for modern and ancient carbonate mud deposition. *J. Sediment. Res.*, 83, 1026–1032.
- Schieber, J. and Wilson, R.D. (2021) Burrows without a trace how meioturbation affects rock fabrics and leaves a record of meiobenthos activity in shales and mudstones. *Paläontologische Zeitschrift*, **95**, 767–791.
- Schratzberger, M. and Ingels, J. (2018) Meiofauna matters: the roles of meiofauna in benthic ecosystems. *J. Exp. Mar. Biol. Ecol.*, **502**, 12–25.
- Schuster, A., Vargas, S., Knapp, I.S., Pomponi, S.A., Toonen, R.J., Erpenbeck, D. and Wörheide, G. (2018) Divergence times in demosponges (Porifera): first insights from new mitogenomes and the inclusion of fossils in a birth-death clock model. BMC Evol. Biol., 18, 114.
- Scoffin, T.P. (1987) An Introduction to Carbonate Sediments and Rocks. Blackie, Glasgow and London, 274 pp.
- Servais, T., Cascales-Minana, B. and Harper, D.A.T. (2021) The great Ordovician biodiversification event (GOBE) is not a single event. *Paleontol. Res.*, **25**, 315–328.
- Shen, Y. and Neuweiler, F. (2018) Questioning the microbial origin of automicrite in Ordovician calathid–demosponge carbonate mounds. Sedimentology, 65, 303–333.
- Shinn, E.A. (1968) Practical significance of birdseye structures in carbonate rocks. *J. Sediment. Petrol.*, **38**, 215–223
- Shirayama, Y. and Kojima, S. (1994) Abundance of deep-sea meiobenthos off Sanriku, northeastern Japan. J. Oceanogr., 50, 109–117.
- Stocchino, G.A., Cubeddu, T., Pronzato, R., Sanna, M.A. and Manconi, R. (2021) Sponges architecture by colour: new insights into the fibres morphogenesis, skeletal spatial layout and morpho-anatomical traits of a marine horny sponge species (Porifera). Eur. Zool. J., 88, 237–253.
- Stock, C.W. and Sandberg, C.A. (2019) Latest Devonian (Famennian, expansa zone) conodonts and spongemicrobe symbionts in pinyon peak limestone, star range, southwestern Utah, lead to reevaluation of the global

- Dasberg event. Palaeogeogr. Palaeoclimatol. Palaeoecol., 534, 109271.
- Szatkowski, T., Kopczyński, K., Motylenko, M., Bormann, H., Mania, B., Graś, M., Lota, G., Bazhenov, V.V., Rafaja, D., Roth, F., Weise, J., Langer, E., Wysokowski, M., Żółtowska-Aksamitowska, S., Petrenko, I., Molodtsov, S., Hubalkova, J., Aneziris, C.G., Joseph, Y., Stelling, A.L., Ehrlich, H. and Jesionowski, T. (2018) Extreme biomimetics: carbonized 3D spongin scaffold as a novel support for nanostructured manganese oxide(IV) and its electrochemical applications. *Nano Res.*, 11, 4199–4214.
- Szulc, J. (1997) Middle Triassic (Muschelkalk) spongemicrobial stromatolites, diplopores and Girvanella-oncoids from the Silesian Cracow upland. In: 3rd IFAA Regional Symposium and IGCP 380 International Meeting, Guidebook, pp. 10–15. University of Cracow, Poland, Cracow.
- Towe, K.M. and Rützler, K. (1968) Lepidocrocite iron mineralisation in Keratose sponge granules. Science, 162, 268–269
- Traunspurger, W. and Majdi, N. (2017) Meiofauna. In: Methods in Stream Ecology, Volume I: Ecosystem Structure (Eds Hauer, F.R. and Lamberti, G.A.), 3rd edn, pp. 273–295. Elsevier, Amsterdam.
- Tucker, M.E. and Wright, V.P. (1990) Carbonate Sedimentology. Blackwell Scientific Publications, Oxford, London.
- **Turner**, E.C. (2021) Possible poriferan body fossils in early Neoproterozoic microbial reefs. *Nature*, **596**, 87–91.
- Turner, E.C., James, N.P. and Narbonne, G.M. (2000) Taphonomic control on microstructure in early Neoproterozoic reefal stromatolites and thrombolites. *Palaios*, **15**, 87–111.
- Villegas-Martin, J. and Netto, R.G. (2018) Permian macroburrows as microhabitats for meiofauna organisms: an ancient behaviour common in extant organisms. Lethaia, 52, 31–43.
- Walcott, C.D. (1917) Middle Cambrian Spongiae. Smithson. Misc. Collect., 67(6), 261–364.
- Wallace, M.W., Hood, A.V.S., Woon, E.M.S., Hoffmann, K.-H. and Reed, C.P. (2014) Enigmatic chambered structures in Cryogenian reefs: the oldest sponge-grade organisms? *Precambrian Res.*, 255, 109–123.
- Wiedenmayer, F. (1978) Modern sponge bioherms of the great Bahama Bank. *Eclogae Geol. Helv.*, **71**, 699–744.
- Wilkinson, C.R. (1978) Microbial associations in sponges. I. Ecology, physiology and microbial populations of coral reef sponges. Mar. Biol., 49, 161–167.
- Wood, R., Zhuravlev, A.Y. and Anaaz, C.T. (1993) The ecology of lower Cambrian buildups from Zuune arts, Mongolia: implications for early metazoan reef evolution. Sedimentology, 40, 829–858.
- Wörheide, G. (2008) A hypercalcified sponge with soft relatives: *Vaceletia* is a keratose demosponge. *Mol. Phylogen. Evol.*, **47**, 433–438.
- Wright, V.P. and Barnett, A.J. (2020) The textural evolution and ghost matrices of the cretaceous Barra Velha formation carbonates from the Santos Basin, offshore Brazil. *Facies*, **66**, 7.
- Wu, S., Chen, Z.-Q., Su, C., Fang, Y. and Yang, H. (2021) Keratose sponge fabrics from the lowermost Triassic microbialites in South China: geobiologic features and Phanerozoic evolution. Global Planet. Change, 211, 103787. https://doi.org/10.1016/j.gloplacha.2022.103787.
- Wulff, J. (2016) Sponge contributions to the geology and biology of reefs: past, present and future. In: Coral Reefs at

Keratose sponges in ancient carbonates

969

the Crossroads (Ed. Hubbard, D.K.), pp. 103–126. Springer Science + Business Media, Dortrecht.

Yang, X.L., Zhao, Y.L., Babcock, L. and Peng, J. (2017) Siliceous spicules in a vauxiid sponge (Demospongia) from the Kaili biota (Cambrian stage 5), Guizhou, South China. Sci. Rep., 7, 42945.

Zheng, L.J., Jiang, H.X., Wu, Y.S., Zhang, Y.-Y., Ren, J.-F. and Huang, Z.-L. (2020) *Halysis* Høeg, 1932 — an ancestral tabulate coral from the Ordos Basin, North China. *J. Palaeogeogr.*, **9**, 26.

Manuscript received 21 March 2022; revision accepted 7 November 2022

# **Supporting Information**

Additional information may be found in the online version of this article:

Table S1. Compilation of publications describing possible keratose sponges, presented in stratigraphic order (oldest at bottom), together with key points and interpretive comments by the authors of this study; the list of references in the table is provided below the table.